university of groningen

faculty of mathematics and natural sciences

Simulating the Influence of Lateralized Reactions in Schooling Fish

Master's Thesis Computer Science

August 31, 2015

Student: Jelle C. Nauta

Primary supervisor: Dr. Michael H. F. Wilkinson

Secondary supervisor: Prof. Dr. Charlotte K. Hemelrijk

Abstract

In this Master's thesis, the influence of behavioral lateralization in schooling fish is studied using an agent-based simulation. For this, we wrote a tool in C++ and GLSL for 3D simulations, with emphasis on extensibility and speed. The fish in our simulations are lateralized by letting them respond more strongly to neighbors on their left than on their right, or vice versa. We first study the behavior of our model without lateralization for school sizes of up to 2000 individuals, and compare these to simulation efforts from the literature. We then study the influence of individual lateralization strength, and of mixing individuals of opposite lateralization in the same school, in schools of 200 simulated fish. Schooling behavior is evaluated using a number of metrics such as nearest neighbor distance, school volume, turning rate and school speed. The most important feature of a lateralized fish in our model is that it has a preferential turning direction (left or right) while schooling. In schools consisting of fish with opposite lateralization directions, this turning preference leads to assortment of fish by their lateralization direction. In schools with unequal fractions of opposite lateralization, we find that the school has a turning bias. This bias leads to several non-monotonic dependencies of our metrics with respect to the ratio of fish with different lateralization types. These non-monotonic dependencies demonstrate that interactions between neighbors in a school may lead to schools that are composed of different numbers of left- and right-lateralized individuals, as observed in nature.

Contents

1. Introduction

In this introduction, we first explain what is meant by individual and population-level lateralization, the topics of our research. We then formulate the research goals and give some background of the method by which we will approach these: agent-based simulation.

1.1 Lateralization

Lateralization is the term used to indicate left-right differences in animal behavior. If lateralization is caused by asymmetry of the nervous system (and in particular the brain), rather than e.g. physical shape, it is referred to as cerebral lateralization. At first believed to be a trait specific to humans, it became clear several decades ago that cerebral lateralization is in fact common in a wide variety of animals. Evidence for cerebral lateralization has been found in several species of fish, amphibians and reptiles (Bisazza et al. [1998]), birds (Rogers [2000], Rogers [2012]) and various mammals such as rats and primates. A comprehensive overview is given by Glick [2012].

In this project we are concerned with lateralization of schooling fish. One of the aims of this project is to find out how the structure and stability of a school depend on the lateralization of its constituent fish. The kind of lateralization that we are concerned with is for fish to respond differently to neighbors on their left side than to neighbors on their right. Several empirical studies have reported such lateralization. Bisazza et al. [1999] found for example that mosquitofish are more likely to perform predator inspection if they have a companion on their left side, rather than on their right side. Bisazza et al. [2001] showed that the males of various species have a preferential eye for inspecting females during sexual behavior, and for inspecting rival males when attacking them. Sovrano et al. [2001] showed that several species spend more time inspecting their mirror image with their left eye than with their right eye.

Considering that cerebral lateralization is so common, it is reasonable to assume that there is some evolutionary advantage to it. It turns out that lateralization of the brain is useful because it allows for better specialized regions in the brain (Levy [1977], Sherry and Schacter [1987]). These brain regions are functionally incompatible, i.e., they would interfere with each other's effectiveness if they were to occupy the same location in the brain (e.g. Rogers [2000]).

The specialization of brain regions may be an accurate explanation for lateralization in schooling fish. It is however conceivable that if fish in a school respond differently to their neighbors on the left than to those on the right, this will lead to a change in the structure of the school as a whole. Such changes in school structure might also affect the evolution of lateralization.

1.2 Population-level lateralization

Lateralization as discussed so far is referred to as *individual* lateralization, and it may vary in strength and direction between individuals. If one direction of lateralization is generally advantageous over the other direction, we might expect all individuals in a population to be lateralized in this same, favorable direction. Alternatively, there might be an advantage to being lateralized in the opposite direction than the majority, for example to be unpredictable for predators. This would put selection pressure on individuals with the majority-type lateralization, so that we would expect one half of a population to be lateralized in one direction and the other half in the other direction.

It turns out that often, populations have a different distribution; a substantial minority is lateralized in the other direction than the majority. A well-known example is handedness in humans, where about ten percent of all individuals is left-handed. The extent to which a population has skewed proportions of left and right lateralization is referred to as *population-level* lateralization.

Population-level lateralization in fish has been observed in several studies: Sovrano et al. [2001] performed experiments with individual fish of various species in mirrored tanks, and observed that on average, the fish more often inspected their mirror image with their left eye than with their right eye. Bisazza et al. [1999] and De Santi et al. [2001] investigated eye-preference in mosquitofish in the vicinity of a predator. They found that individual mosquitofish have an eye-preference for inspecting a predator, with a population-level bias: about 75% inspect the predator with their left eye, and the rest does the opposite. The mosquitofish were also more likely to perform predator inspection when they perceived their mirror image on their left side rather than on their right side. An in-depth treatise of population-level lateralization is given by Møller and Swaddle [1997].

Besides investigating the influence of individual lateralization in fish schools, this project aims to study how population-level lateralization influences the school. While the causes of individual lateralization are well explained, the causes of lateralization at the population-level are still debated. One possible explanation is proposed by Vallortigara and Rogers [2005]. They argue that a population bias may arise due to evolutionarily stable strategies that result from a balance of conflicting cost functions.

As an example consider a school of prey fish, as theoretically treated by Ghirlanda and Vallortigara [2004]. Belonging to a minority of prey fish may give an advantage in evading predators for whom it is better to specialize in hunting the majority type. However, belonging to the minority type may also give a disadvantage in predator evasion. This is because it may lower the chances of staying together with a group of conspecifics, who are also more used to coordinating their movement with majority type neighbors. This is disadvantageous because it reduces the well-known 'safety-in-numbers' of schooling fish. The unpredictability to predators and the 'safety-in-numbers' may both be represented by some cost function that depends on the size of the minority fraction. The cost of being predictable increases with fraction size, the cost of 'unsafety-in-smaller-numbers' decreases with fraction size. Depending on the shapes of these cost functions, a stable minority fraction may be reached, for which fitness is reduced if the fraction becomes any larger or smaller. The sum of both cost functions will have a minimum for this equilibrium size of the minority fraction.

Empirically, it has been found that population-level lateralization is significantly more common in gregarious species than in non-gregarious species (Bisazza et al. [2000]). This finding strengthens the hypothesis that population-level lateralization is indeed caused by an equilibrium of cost functions that depend on interactions with neighbors.

Unfortunately, the hypothesis provides little information on the existence and importance of its supposed competing cost functions, on which it critically depends.

1.3 Research goals

Given the supposed advantages and disadvantages of being lateralized in a school as proposed by Ghirlanda and Vallortigara [2004], it is of great interest to know *how* these advantages and disadvantages would come about. As long as we do not know what effect lateralization has in practice, it is hard to tell whether population-level lateralization is really caused by competing cost functions.

How do the characteristics of the school change as a result of lateralization of individual fish? And does population-level lateralization cause a difference in circumstances for the minority and majority? The minority and majority may for example occupy different locations in the school, or have different probabilities of being separated from the school.

In this project, we try to answer these questions. As explained in the next section, we use an agent-based simulation for this. Exploratory simulations with lateralized schools were done in NetLogo, a Java-based tool for agent-based simulations. NetLogo allows only for 2D simulations, which may not capture the dynamics of real fish schools sufficiently. NetLogo also proved to be too slow for our purposes. We therefore need to write our own tool for 3D agent-based simulations. Program requirements and design will be discussed in section 2.3.

1.4 Agent-based simulation

To investigate the influence of lateralization on fish schools, we could take several approaches:

1. **Empirical study of fish in a laboratory**. This is the most realistic, but also difficult and time-consuming.

2. **Abstract mathematical analysis** (similar to the work of Ghirlanda and Vallortigara [2004]). This could give very elegant and general results, but makes it difficult to incorporate individual behavior and local interactions.

3. **Agent-based simulation**. This does not abstract as much as pure mathematical analysis and allows school structure to emerge from individual behavior. In this sense, it is more realistic than abstract mathematical analysis. In contrast to empirical study, it allows full control over (and information on) the school. This makes it easy to gain more insight into the model by changing some parameters and observing the result.

We decide to use an agent-based simulation. This makes the work manageable in our timeframe and allows us to model the school at the level of individual fish, as seems appropriate for modeling lateralization.

Schooling behavior has been extensively studied using agent-based models. The application of agent-based simulations to lateralization is however, to the best of our knowledge, new in this project. In the rest of this section we give an overview of the existing literature on agent-based simulation of fish schools.

The models used in the literature are very diverse, ranging from 2D cellular automata for investigating swimming efficiency and oxygen depletion (Stöcker [1999]) to 3D simulations using hundreds of thousands of individuals in predator-prey scenarios (Solar et al. [2011]). Most of the research appears to use relatively small schools, with up to 100 individuals. Notable exceptions are Hemelrijk and Hildenbrandt [2008], who study the influence of school size (up to 2000 individuals) on the density distribution within the school, Vabø and Skaret [2008], who simulate a group of up to 8000 spawning herring, and Solar et al. [2011], who mainly intend to demonstrate the possibility of simulating very large schools (up to 320.000 individuals).

Almost all simulations use forward Euler integration to simulate the time-evolution of the system. Also, all models include cohesion (the tendency of fish to move toward each other) and some form of repulsion (the tendency to move apart). Without these interactions, realistic schooling is hard to imagine. Most models also include

an alignment interaction (Huth and Wissel [1992], Huth and Wissel [1994], Stöcker [1999], Couzin et al. [2002], Parrish et al. [2002], Viscido et al. [2005], Kunz and Hemelrijk [2003], Hemelrijk and Kunz [2005], Hemelrijk et al. [2010], Solar et al. [2011]), but some do not (Warburton and Lazarus [1991], Romey [1996], Vabø and Skaret [2008]). It appears that without an explicit tendency for individuals to align their forward direction, coordinated movement of the school can only emerge in very small schools (<15 individuals) of fish swimming at the same, constant speed and having a suitable attraction/repulsion function (Romey [1996]).

In some models, all fish have the same speed (Romey [1996], Stöcker [1999]), or all fish have constant speeds that vary per individual (Couzin et al. [2002]). Some models let fish change their speed randomly in each time step (Huth and Wissel [1992], Kunz and Hemelrijk [2003]), and some let fish change their speeds depending on their neighbors. The latter is the most biologically realistic approach (Katz et al. [2011]).

Turning and acceleration are often treated separately, but in some research they are unified by treating individual fish as particles that interact through Newtonian forces (Parrish et al. [2002], Vabø and Skaret [2008], Hemelrijk et al. [2010]). This is a conceptually elegant way of treating a special combination of turning and acceleration dependencies.

The usual way in which interactions with neighbors are integrated is by (weighted) averaging of response vectors, although the weighing scheme differs between models. It may depend for example on distance and relative angle to the neighbor. In this respect there are also different approaches: the model of Couzin et al. [2002] is rule-based, with alignment and attraction only being considered when no repulsion occurs (although we could think of this as assigning infinite weight to separation). Vabø and Skaret [2008] used a rule-based approach in which a fish sequentially applies different types of interactions (depending on fixed priorities), and once maximum acceleration is reached, the remaining interactions are ignored.

There are many more differences in the way schools are modeled, but it should be clear from the above that there is no standard schooling model. Parrish et al. [2002] provide an excellent overview of some of the key differences between various models from the literature and demonstrate that different choices for the model often lead to differences in schooling behavior. It is important to keep this in mind: results from a single model may generalize badly and should be replicated in multiple frameworks to see how resilient they are to changes. Ideally, one would of course compare any results to empirical data on various species. However these are unfortunately scarce because they are difficult and costly to obtain, and the requirements of the data are often very specific to the research question.

Model parameters that are studied in the literature are varied. Examples include individual differences in speed, turning rate, shape and size of interaction zones, number of influential neighbors and the presence of 'leaders' in the school. Emergent phenomena are the shape and velocity of the school, assortment based on individual differences, state-transitions in schooling behavior and, in the case of Vabø and Skaret [2008], even the formation of 'bridges' connecting the top and bottom regions of a school of spawning fish.

It should be noted that although agent-based simulations have been extensively used to study fish schools in the past, the application to lateralization is, to the best of our knowledge, new in this project.

2. Methods

2.1 Agent-based simulation

Our simulation is in many respects similar to that of previous studies. The school of fish is represented at the level of the individual fish. Each simulated fish perceives the other individuals in its vicinity, and regulates its movement based on their positions and orientations. Since an analytical solution of the differential equations that arise from this system is very difficult (not to say impossible), we use a numerical method to calculate the evolution of the system. There are various integration methods we could use for this, and we decide to use a very simple method: forward Euler integration. Other methods, such as higher-order explicit or implicit Runge-Kutta methods are more accurate, but slower. Since our system is a non-trivial many-body problem, we expect the trajectories of individual fish to be chaotic (for the relation between N-body problems and chaos, see for example Roy [2012]). It would therefore be a wasted effort to solve the movement of individual fish with high accuracy.

2.2 Model specification

2.2.1 Fish model

Spatial representation

Each fish has a 3D position (the coordinates of the fish in the global frame of reference) and an orientation (the rotation of the fish, defining its forward and up directions). Position and orientation can be represented together into a single transformation called the *pose*. It is possible to represent the pose by a single 4×4 matrix, but this makes it difficult to correctly apply rotations and translations separately. Therefore, position and orientation are each represented by a separate 4×4 matrix. Such matrices are frequently used in computer graphics and robotics to represent rotations and translations. See for example sections 5.2 and 11.2 of Hearn and Baker [1997].

We denote the position vector of a fish A as r_A. The vector from fish A to fish B is then denoted as $\mathbf{r}_{AB}$, with $\mathbf{r}_{AB} = \mathbf{r}_B - \mathbf{r}_A$. The distance between fishes A and B is denoted as $d_{AB} = \|\mathbf{r}_{AB}\|$.

The orientation of a fish A is determined by its forward-vector $\mathbf{e}_{x,A}$, its up-vector $\mathbf{e}_{y,A}$ and right-vector $\mathbf{e}_{z,A}$. For an unrotated fish these vectors are aligned with the x, y and z-directions of the global frame.

The fish model we use for visualization has length 1, height 0.3 and width 0.3. The only theoretical consequence of this is that our unit of distance is the body length (BL), which is important for defining (and understanding) our parameters and comparing results with the literature. The program does not perform any collision tests, so the size and shape of the fish is irrelevant in this regard. We do set the parameters in such a way that collisions between fish are very rare as is verified by visual inspection.

Field of vision

Fish have many sensory systems, but it is generally assumed that the two main ones used for schooling behavior are:

1. Eyes: fish usually have their eyes on either side of the head, so that their visual field of view is quite large, with a relatively small blind angle behind them.

2. Lateral line: on both sides of the body, fish have a longitudinal sensory organ with which they can perceive vibrations in the water.

Visual input is mostly important to regulate relative positioning, while the lateral line is mostly important for monitoring the relative swimming direction of neighbors, as well as their speed (Partridge and Pitcher [1980]).

Since we want to model lateralization, we separate the “sensory systems" into a left and a right region. A region is defined by a maximum distance at which a fish can perceive a neighbor, and two angles θ and ϕ. See figure 2.1.

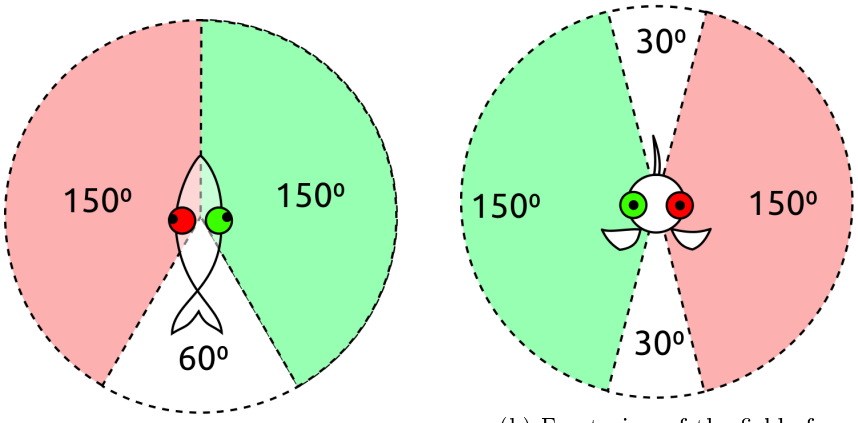

(a) Top-down view of the field of view of a fish. Neighbors in the red area are considered left neighbors, neighbors in the green are are right neighbors.

(b) Front view of the field of view of a fish. Neighbors in the grey areas are visible, the fish has blind angles above and below it. Note that in 3D, the blind areas are cones, not wedges.

Figure 2.1: Field of view of a fish.

The angle θ defines the field of view in the xz-plane of a fish (the plane normal to the up direction of the fish). With $\theta = 150°$, the fish perceives neighbors in front of it in a symmetrical region ranging from $-150°$ to $150°$, with a blind angle of $60°$ behind the fish.

The angle ϕ defines the vertical angle in which a fish may perceive neighbors. This is also defined to be symmetrical, so that the vertically visible angle ranges from $-\phi$ to $+\phi$. We set ϕ to $75°$, so that the fish have a blind angle of $30°$ above and below them.

Furthermore, there is a maximum distance $d_{\max}$ at which a neighbor can be perceived. Together, this means that a neighbor B is visible to fish A if and only if

$$|\theta_{AB}| < \theta \qquad \text{and} \qquad |\phi_{AB}| < \phi \qquad \text{and} \qquad d_{AB} < d_{\max},$$

where

$$\theta_{AB} = \text{atan2}(\mathbf{r}_{z,AB}, \mathbf{r}_{x,AB})$$
$$\phi_{AB} = \text{atan2}(\mathbf{r}_{y,AB}, \sqrt{\mathbf{r}_{x,AB}^2 + \mathbf{r}_{z,AB}^2}).$$

Depending on the model (as detailed in chapter 3), for each fish there is set of visible neighbors determined to which it will respond in the current time step. From the relative positions and orientations of these neighbors, a turning response and speed change are calculated.

Simulated mechanism of lateralization

Although empirical data on lateralization are abundant, these data are mostly observational; they give no insight into the specific mechanisms that could explain the observations. We therefore decide on a very simple mechanism. Each fish responds to a number of nearby neighbors and combines the reactions to multiple neighbors by weighted averaging. Lateralization is achieved by giving the positional reaction to a neighbor on the left a different weight than the reaction to a neighbor on the right. The reason we only lateralize the positional interaction, and not also the alignment and speeding interactions, is that this keeps the model simpler and makes the analysis easier.

The left and right weights of neighbor interactions sum to one, see figure 2.2. The lateralization parameter λ ranges from zero to one and has an intuitive interpretation: for $\lambda = 0$, neighbors from both sides are considered equally important; there is no lateralization. For $\lambda = 1$, neighbors from one side are ignored; this corresponds to maximum lateralization.

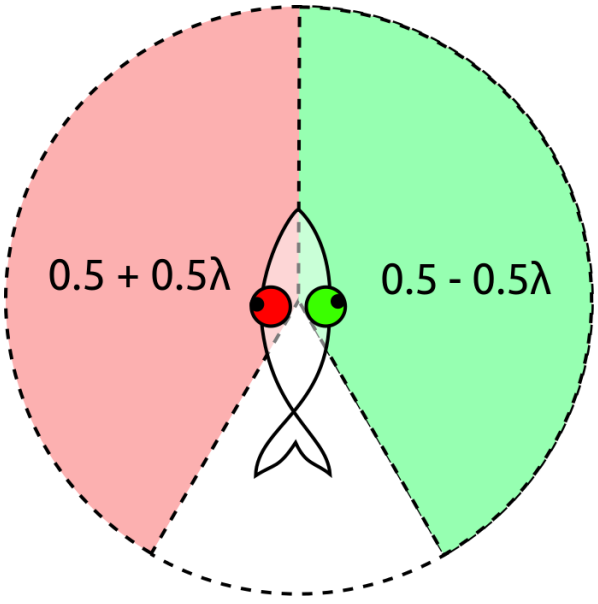

Figure 2.2: The weights that a left-lateralized fish assigns to reactions from neighbors on the left and on the right. In a right-lateralized fish, the left and right weight are switched.

The way in which influences from neighbors are combined will be further discussed in the rest of this section.

Turning response

Each fish in our model responds to its neighbors through two types of turning interaction: a positional interaction and an alignment interaction. The positional interaction is based on the relative position of a neighbor, and it is used to regulate the distance between fish. The alignment interaction, based on the relative forward direction, compels fish to move in the same direction. It is used to achieve schooling, rather than chaotic shoaling.

The net response of a fish is calculated by first determining individual responses to all influential neighbors. The positional and alignment responses each have their own, fixed angle. All positional response vectors therefore lie on a cone around the current forward-vector of the focal fish, and the same holds for the alignment responses (be it on a different cone). The integration of responses from multiple fish is done by taking the weighted average of all these response vectors. Since the turning angles of responses are fixed, the relative impacts of responses are determined by the weight factors associated with the responses. Weight factors are based on how important a certain response is supposed to be to the fish. The advantage of this approach over using angle size to determine relative importance is that we can make a single contribution arbitrarily important while keeping a clear bound on the maximum turning rate.

Consider a fish A, responding to neighbor B. The rotational axis $\mathbf{n}_{AB}$ of its positional interaction is calculated as $\mathbf{n}_{AB} = \mathbf{e}_{x,A} \times (\mathbf{r}_B - \mathbf{r}_A)$. For a positive angle, A rotates toward B and with a negative angle, A rotates away from B. To decide which direction to turn, we define an equilibrium distance d_{eq} that each fish should try to maintain to its neighbors. If neighbor B is further away, A turns toward it, if B is closer, A turns away from B. It would be simplest to always use a weight of 1 for the positional interaction, but as our early experiments revealed, this easily leads to chaotic schools. A better approach is to let the weight gradually increase as the deviation of the distance from the equilibrium distance increases (as is customary in schooling models, Warburton and Lazarus [1991] give a theoretical justification, Katz et al. [2011] provide empirical evidence). We choose the weight w of the positional response of individual A to a selected neighbor B as the piecewise linear function:

$$w_{\text{positional},AB} = \begin{cases} 10(1 - d_{AB}/d_{eq}) & 0 < d_{AB} \leq d_{eq} \\ d_{AB}/d_{eq} - 1 & d_{eq} < d_{AB} \leq 2d_{eq} \\ 1 & 2d_{eq} < d_{AB} < d_{max} \end{cases} .$$

If a fish has a neighbor that is within a certain distance which we call the 'alignment distance', it is not only influenced through a positional interaction, but also through an alignment interaction. The alignment response is a fixed rotation toward the forward direction of the neighbor, around the rotational axis $\mathbf{m}_{AB} = \mathbf{e}_{x,A} \times \mathbf{e}_{x,B}$. For the averaging over neighbor responses, the alignment response always has weight one. If a neighbor causes both a positional and an alignment interaction, we see these as two separate responses, each with their own weight. See figure 2.3 for a 2D-representation of the different positional interaction zones.

In the context of turning, the following also has to be taken into account:

1. After several rotations, the up-direction of the fish may change in an unwanted way. To counter this, after every time step the up-direction is rotated around the forward-vector of the fish until the right-vector is horizontal.

2. After several time steps, the rotation matrices of the fish may not represent pure rotations anymore, due to round-off errors, introducing skew and scaling.

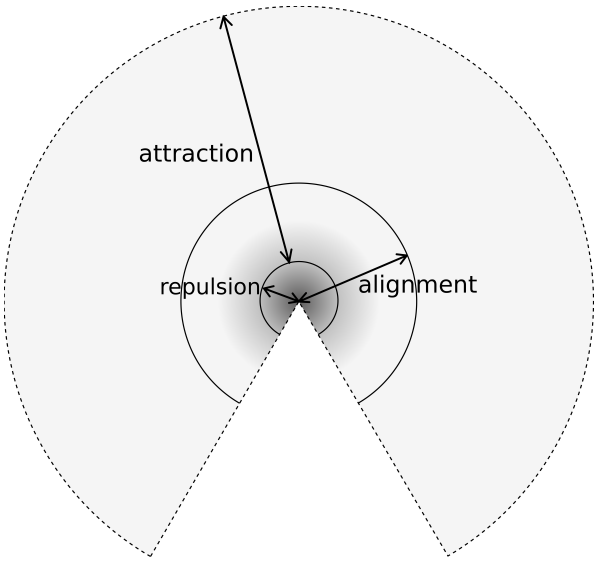

Figure 2.3: Positional and alignment interaction zones. Fish inside the centermost circle have a repulsive influence (dark shading), fish that are outside are attractive (light shading). The gray shading indicates the weight of the positional interaction.

This is countered by performing Gram-Schmidt orthogonalization of the rotation matrices every 10 time steps.

Speed change

Each fish has the same preferred speed, and all fish have that same speed at the start of a simulation. To keep up with neighbors that are far away and to avoid collisions, fish change their speeds (Katz et al. [2011]). If a fish moves at a higher or lower speed than its preferred speed, it experiences an acceleration proportional to the difference between the preferred speed and its current speed.

Like turning interactions, speeding interactions are calculated in each time step as responses to a set of influential neighbors. A speeding response depends on the relative position of an influential neighbor and on the neighbor's speed. We define four speeding interaction zones, see figure 2.4. A fish only responds with acceleration or deceleration to a neighbor if the neighbor is in one of these zones.

1. Far in front: a neighbor is more than distance d_f in front and more in front than sideways or up/downwards; in this case the fish accelerates to catch up.

2. Near in front: a neighbor is less than distance d_n in front and within a certain radius; in this case the fish slows down to avoid collision.

3. Near behind: a neighbor is less than d_n behind and within a certain radius; the fish accelerates to avoid collision.

4. Far behind: a neighbor is more than d_f behind and more behind than sideways or up/downwards; the fish slows down to wait for the neighbor.

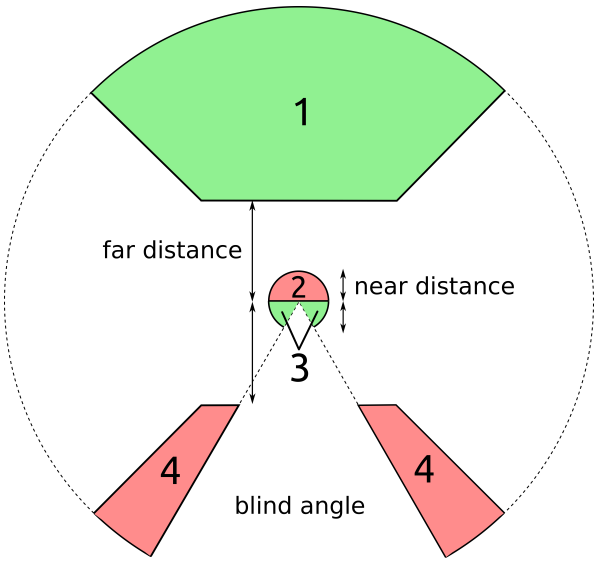

Figure 2.4: Speeding interaction zones: neighbors in the green areas lead to speeding up, neighbors in the red areas result in slowing down. The front and rear acceleration zones are defined to be symmetrical except for the blind angle.

The magnitude of acceleration does not depend on the exact position of the neighbor, only on its speed. We calculate individual speeding responses of a fish to all its influential neighbors. These individual responses are integrated as follows:

1. If at least one of the responses is negative (causing deceleration), the final response is chosen to be the most negative of all responses. This ensures that a fish gives most priority to avoiding collisions with a neighbor in front of it, as well as waiting for neighbors that fall behind.

2. If all responses are non-negative, the final response is chosen to be the most positive one. The reason for this choice is that a fish responds well if it gets a strong acceleration impulse (this impulse could be 'diluted' if we used averaging). It also prevents acceleration from being too high (this could happen if we summed all speeding responses and the focal fish got several strong acceleration impulses at the same time).

An individual speeding response is a constant acceleration (positive or negative) multiplied by the speed of the neighbor that the focal fish reacts to. This dependence on neighbor speed is based on experimental observations from Katz et al. [2011]. Compared to the burst-and-coast accelerations of at least 3 BL s^{-2} in Cod and Saithe as found by Videler and Weihs [1982], our accelerations are around an order of magnitude lower. The reason we did not choose this value higher is that it resulted in undesired schooling behavior, with erratic acceleration and deceleration. This may have to do with the short time period (around 100 ms compared to our 50 ms time step) in which the fish accelerate, but perhaps a better explanation is that they are incomparable to our simulated fish; real fish experience viscous drag, proportional to their velocity. Therefore, they need to have constant propulsion to keep moving at their preferred speed (a preferred speed that also likely varies). Deceleration is achieved simply by stopping to swim, while acceleration is achieved by actively swimming faster. This

asymmetry likely means that deceleration and acceleration differ in magnitude and have different speed dependence than the symmetric deceleration and acceleration in our model. Furthermore, our simulated fish do not have a burst-and-coast strategy (like the real fish studied by Videler and Weihs [1982].

Short experiments revealed that schooling behavior is very sensitive to changes in the parameters of the speeding interaction; disabling speeding interaction zones (see figure 2.4) has some interesting effects:

1. If we disable the far front zone, the school becomes very elongated, and the tail will quickly break away.

2. If we disable the near front zone, the rear fish avoid collision with the fish in front of them only through turning. Because of this, the school becomes very short.

3. If we disable the near rear zone, a narrow tail sometimes develops, since fish at the rear can no longer 'push' the fish in front of them, so that they have difficulty in merging with the bulk of the school.

4. If we disable the far rear zone, a notable increase in 'flaking' away of the front occurs: fish at the front escape a short distance, and then turn toward one side through attraction. They then swim along the school in the opposite direction until they align again. The far rear zone prevents this by slowing them down so that they stay in the school, thereby lowering the chance of flaking.

The distance at which interaction zones are placed is also important. In particular, the extent of the near zone has a big influence on the number of neighbors that reach that zone, since the positional interaction may steer them away in time. The degree of order in the school also influences this process, since in more disorderly schools, fish are more likely to get closer to each other. This means that the speeding interaction is inseparably coupled with many other parameters and mechanisms of the model.

With these fine dependencies in mind, we choose the acceleration settings in such a way that they result in stable, visually satisfactory schooling behavior.

Movement noise

To somewhat realistically model random changes in direction by the fish, we took inspiration from Gautrais et al. [2009] to model the fish as persistent turning walkers. Each fish has a turning bias; apart from its usual turning due to neighbor interactions, in every time step a turning bias is added to its rotation. We could draw this bias from a random distribution in every time step, as done by e.g. Warburton and Lazarus [1991]. The obvious drawback of this is that noise quickly averages out, and increasing noise leads to erratic turning between time steps.

A better approach is to give each fish a state variable representing its bias. We add a randomly drawn change to this bias in every time step, clipping the bias in a fixed range around zero to prevent it from becoming too large. This way, an individual bias does not change too drastically between time steps, but it can still be a sizeable contribution to the turning of a fish. An isolated fish will therefore swim along a curved path so as to simulate searching behavior. Since we treat yaw and pitch separately, we use a separate turning bias for each.

We must take some care to make a turning bias independent of the time step. For example, if we were to draw changes to the bias from a uniform distribution, we would get very different outcomes if we drew from [-1, 1] for a time step of 30 ms than

if we did the same for 60 ms. The influence of noise would clearly be much stronger for a time step of 30 ms. Of course, drawing from [-0.5, 0.5] for 30 ms would not solve the problem since the sum of two uniform variables is not uniformly distributed.

The solution for this is to use a Gaussian distribution. Since sums of Gaussian distributions are also Gaussian, and we are only concerned with zero-mean distributions, we only need to set the variance based on the time step. The sum of two Gaussians with variances σ_X^2 and σ_Y^2 has variance $\sigma_Z^2 = \sigma_X^2 + \sigma_Y^2$. Therefore, we simply let the variance of our distribution scale linearly with the size of our time step. Finally, for a time step that is twice as large, we wish to allow twice the maximum rotation bias per time step. Therefore we also stretch the range of allowed rotations linearly with the time step.

2.2.2 World size

The fish in the model move in a cylinder with Euclidian topology. The cylinder is infinite (for all practical purposes) in the y-direction, i.e., up. Alternatively, we could use a toroidal topology, but this would make calculating distances much more involved, and we choose to avoid this.

A disadvantage of the xz-bounded Euclidean world is that the fish are repelled by the boundary, which disturbs the school and thus influences the data. To mitigate boundary effects, the world is made fairly large by giving it a radius of 10000 BL. One concern is that the school might constantly follow the boundary, moving in very large circles. To prevent this, we use a ring-shaped boundary region of 200 BL wide. When a fish passes through this ring and reaches the outside region, it gets a turning bias toward the center of the world. This turning bias is disabled again once the fish is back in the inner region. This way, fish always make 180°turns near the boundary, rather than small adjustments that would let them swim in large circles along the border.

Note that in principle we could make the world infinitely large. One consequence is that once the school disintegrates, the chances of fish encountering each other again would be quite small. Another reason for us to limit the world is to facilitate nearest neighbor searching, as explained in the next subsection.

2.2.3 Neighbor search

A fish in a school only interacts locally, and we wish to find its nearest neighbors. A brute-force search would take time quadratic in the number of individuals, which would be prohibitively slow - we must use a different approach. There are many algorithms in the literature for K-nearest neighbor search. Most of these are intended for static data points and use R-trees or variations thereof (e.g., Roussopoulos et al. [1995], Korn et al. [1996], Seidl and Kriegel [1998]). The rise of mobile computing brought more attention to K-nearest neighbor search in dynamic data. Kalashnikov et al. [2004] and Yu et al. [2005] both found that for K-nearest neighbor searches *among moving agents*, their grid-based algorithms were faster than R-tree based methods. This indicates that a grid-based method may be best suited in our case. Another argument for using a grid-based search is that these are in general easier and faster to implement than R-trees. We therefore choose to use a simple box search which resembles the one described by Zhao et al. [2013]. This approach was also taken by Vabø and Skaret [2008] for the neighbor search in their simulations with up to 8000 spawning herring. We will now describe how our box search works. The time complexity of the algorithm will be discussed in section 4.1.

Our box search algorithm

For the box search, the space in which the fish are allowed to swim is divided in a grid along the x- and z-dimensions. The fish mostly stay in the xz-plane, so we choose not to divide the space in the y-direction, to save memory (as stated above, the world has to be fairly large). The world is thus represented by a 2D-array of boxes, with each box containing a list of the fish that currently occupy it. Determining which box a fish occupies is easily done by multiplying its coordinates with some factor and rounding down. The result is then used as indices in the array.

If we wish to find the nearest neighbors of a fish, we only have to inspect some boxes in its vicinity. Say we want to find the single nearest neighbor. Starting at its own box, we may already find a neighbor. We store the minimum distance, to the closest neighbor in this box. However, since our fish may be on the edge of its box, there might be a neighbor in one of the surrounding boxes that is nearer. Call the length of a box side L. After checking the region of 3×3 boxes around the fish, we know for sure that any neighbors that we have not yet found are at a distance of at least L. If we have found any neighbor at a smaller distance, we know for sure that one of them is the nearest neighbor and can stop our search. If not, we still have to search further outward. To keep the solution generic, we keep inspecting rings of boxes as we go outward. After the second ring we have searched a region of 5×5 boxes, and know that any unseen neighbors are at least at a distance of $2L$.

One subtlety that arises is that we need to store neighbors of inner rings that may or may not be *nearest* neighbors, and somehow decide when one of the neighbors found so far is the nearest. The neighbors found in the searched region are all stored in an array (using pointers). To determine when to stop searching, two numbers are maintained during the search:

1. The number of neighbors found that are definitely nearest (in fact, a lower bound on this). After checking the first box, this number is still zero since any neighbors in the first ring may be arbitrarily close.

2. The number of neighbors that may be further away than some neighbors in the next ring, but are definitely closer than those in the ring after that.

Every time we search the next ring, the second number is added to the first.

Assuming a box side of 1 (the adaptation to other side lengths is trivial), the following pseudocode describes the search.

Listing 2.1: Algorithm for finding nearest neighbors.

```
function searchRings
  input:
    F, the fish whose nearest neighbors we want to find
    N, the number of nearest neighbors to find
    B, the boxgrid (implicitly used to search rings)
  output:
    neighborsFound, a set of neighbors, of which the
      N closest ones are F's N nearest neighbors.

  ringIndex = 0
  withinThisRing = 0
  withinNextRing = 0
  neighborsFound = empty set
  ringNeighbors = empty set
```

```
  while withinThisRing < N do
    withinThisRing = withinThisRing + withinNextRing
    withinNextRing = 0
    ringNeighbors = neighbors in ring ringIndex
    add ringNeighbors to neighborsFound
    for neighbor in ringNeighbors do
      if distance(F, neighbor) < ringIndex do
        withinThisRing = withinThisRing + 1
      else if distance(F, neighbor) < ringIndex + 1 do
        withinNextRing = withinNextRing + 1
      end if
    end for
    ringIndex = ringIndex + 1
  end while
  return neighborsFound
end
```

To better understand how the search works, consider figure 2.5. Let us find the 2

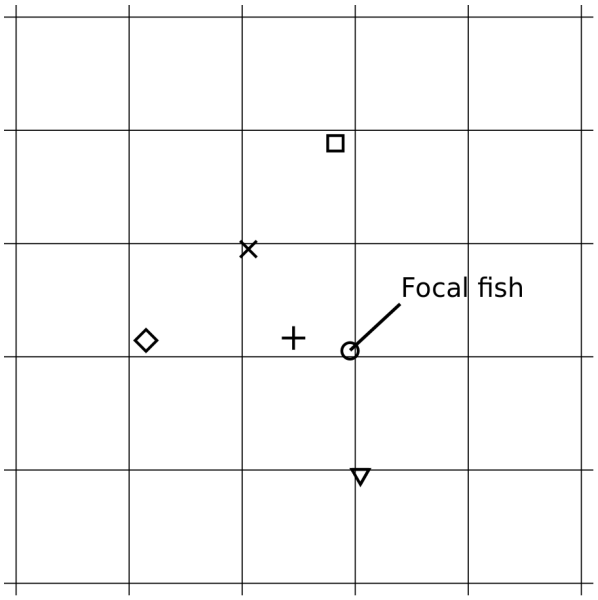

Figure 2.5: Illustration of nearest neighbor search.

nearest neighbors of the focal fish represented by ○. After checking the first box (ringIndex = 0), × and + have been added to `neighborsFound`. Since + is within distance ringIndex + 1 = 1 (and × is not), `withinNextRing` is now one.

When we start checking the first ring of boxes (`ringIndex` = 1), we first add `withinNextRing` to `withinThisRing` and reset `withinNextRing` to 0. Consequently, `withinThisRing` is now 1. Note that × was only added to the set `neighborsFound`, but is not used for the stopping criterion. After checking the first ring, ◇ and □ have both been added to `neighborsFound`. Since both are between distances `ringIndex` = 1 and `ringIndex` + 1 = 2, `withinNextRing` is set to 2.

When we start checking the second ring, `withinThisRing` becomes 3, and we reset `withinNextRing` to 0. We add ▽ to `neighborsFound`, and since its distance to ○ is less than `ringIndex` = 2, `withinThisRing` is once more increased, to 4.

After this, the loop terminates since `withinThisRing` > 2, and we return the set of all symbols found so far. This set contains the two nearest neighbors, ∇ and $+$.

For simplicity, the above algorithm does not include the stopping criterion when the maximum vision distance is exceeded, but our model does incorporate this. Also, in our model, the above method is adapted to the restricted viewing angles of the fish; we search for nearest neighbors for both eyes.

The size of a cell in the x- and z-dimensions may be based on two factors:

1. The average distance between fish in a school
2. The visual distance of the fish

The first determines how many fish we are likely to encounter within a single box. We do not want this number to be too high, so the boxes should not be too big. The second determines how many boxes we will have to search if there are no nearby fish. For this reason, the boxes should not be too small, especially when we expect many fish with few neighbors. Another reason for this is that with smaller boxes, the world will contain more boxes and take up more memory. We empirically determined that taking a box size of about the preferred nearest neighbor distance between fish works well for our typical simulation setting.

2.2.4 Metrics of fish schools

Every 10 simulated seconds, a snapshot of all individuals is recorded. We refer to such a snapshot as a 'data step'. From these data steps, the following metrics are computed to quantitatively compare schooling behaviors.

- **Nearest neighbor distance**: for each fish, we calculate the distance to its nearest neighbor.
- **School volume**: for each data step we calculate the alpha shape of the school with $\alpha = 1/4$. This means that two fish are connected if their distance is at most twice the preferred nearest neighbor distance. The advantage of the alpha shape over the convex hull is that with larger schools, any concavities in the school (during turning for example) are not added to the volume. Loosely speaking, the alpha shape tolerates concavities up to size $1/\alpha$. For fixed school size, the volume of the alpha shape also serves as an inverse measure of density. It is a useful metric to compare with nearest neighbor distance in this respect.
- **Polarization**: this measures how well the fish are aligned with each other. To calculate it, we take the average of the forward vectors of all fish. The polarization is then defined as the length of this average vector. Mathematically, for a school of S individuals:

$$\text{Polarization} = \|\frac{1}{S}\sum_{i=1}^{S}\mathbf{e}_{x,i}\|.$$

- **Frontality**: this measures where the core is located in the longitudinal direction of the bounding box. The core is defined as the top 10% individuals with lowest nearest neighbor distance. Its location is defined by its center of mass, which we denote by M_{core}. The bounding box is defined as follows: we first take the average of the forward vectors of all fish. From this, we drop the y-component (up), and use the result as the first, longitudinal axis for the bounding box. The

size of the bounding box in this direction is always referred to as the *length* of the bounding box. The second axis of the bounding box is the y-axis, and the size of the bounding box in this direction is defined to be its *height*. The third axis is defined to be normal to the first two axes, and corresponds to the *width* of the bounding box. The bounding box of the school is the smallest cuboid with these axes that contains all fish in the school. We denote the center of mass of all fish in the school by M, the length of the bounding box by L and the forward direction of the bounding box by $\mathbf{e}_{x,\text{boundingbox}}$. Mathematically, the frontality of the core is then defined as:

$$\text{Frontality} = 0.5 + \frac{1}{L}(M_{\text{core}} - M) \cdot \mathbf{e}_{x,\text{boundingbox}}.$$

If the core is located at the back of the bounding box, the frontality has a value of 0. If the core is at the front, the frontality has value 1, and the frontality linearly ranges between these extremes. The metric closely resembles the one used by Hemelrijk and Hildenbrandt [2008], except that we base our density estimate purely on nearest neighbor distance, instead of also on the number of neighbors in a local neighborhood. The details of the density estimate are not explained by Hemelrijk and Hildenbrandt [2008].

- **Length-over-width ratio** of the bounding box of the school, where the bounding box is defined as for frontality. This measures how oblong the school is in the direction of motion, and was also used by Hemelrijk and Hildenbrandt [2008].

- **Width-over-height ratio** of the bounding box of the school, where the bounding box is defined as for frontality.

- **Relative movement**: unlike the static measures above, relative movement depends on the time-evolution of the school. For each fish, we record the relative positions of the three closest neighbors. In the next measured data step (10 simulated seconds later), we again record the relative positions of these individuals (which need no longer be nearest neighbors). The relative movement is then defined as the mean displacement distance of these three neighbors, averaged over all fish that we take into account, averaged over all subsequent pairs of data steps.

  Some testing revealed that if we include all fish, relative movement is dominated by individuals that break away from the front of the school and join again at the end. Although this is certainly legitimate relative movement in terms of the above definition, we are more interested in the relative movements of fish inside the school during 'normal' swimming behavior. For this reason, we discard the 10% of individuals with the highest contribution to relative movement.

- **Left/right separation**: in lateralized schools, we observed a separation of the left and right lateralization types, with the left lateralized fish tending to the right, and the right lateralized fish tending to the left. To quantify this separation, we calculate the center of mass of all left-lateralized individuals, and of all right-lateralized individuals. We subtract the vector to the center of mass of the school as a whole from the vectors to both these centers of mass. This gives us the position vectors of the two groups, relative to the center of mass of the school. Taking the inner product of the left group with the right-vector of the school $\mathbf{e}_{z,\text{school}}$ gives us a measure of how much a group is separated from the rest. We do the same with the right group, except taking the inner product with

the left-vector $-\mathbf{e}_{z,\text{school}}$. To combine the two measures from both groups, we take the average, weighted with the number of individuals in the corresponding group. Note that high left/right separation means that left-lateralized fish end up on the right of the school, and vice versa for right-lateralized individuals.

- **Turning rate**: the rate of change in the direction of the school, calculated in the xz-plane. For this we calculate the mean forward vector $\mathbf{v}$ of the school for each data step t. Denote the $x-$ and $z-$components of this vector as v_x and v_z. The angle $\theta(t)$ of $\mathbf{v}$ in the xz-plane is then calculated as

  $$\theta(t) = \text{atan2}(-v_z(t), v_x(t)).$$

  We calculate the turning angle $\eta(t)$ of the school for each pair of subsequent angles $\theta(t-1)$ and $\theta(t)$. We must take some care to correctly calculate the turning angle at the $(0, 2\pi)$-gap:

  $$\eta(t) = \begin{cases} \theta(t) - \theta(t-1) + 2\pi & \theta(t) < \frac{1}{2}\pi \text{ and } \theta(t-1) > \frac{3}{2}\pi \\ \theta(t) - \theta(t-1) - 2\pi & \theta(t) > \frac{3}{2}\pi \text{ and } \theta(t-1) < \frac{1}{2}\pi \\ \theta(t) - \theta(t-1) & \text{otherwise.} \end{cases}$$

  The turning rate metric is the average of the absolute values of all these angles:

  $$\text{turning rate} = \frac{1}{T-1} \sum_{t=2}^{T} |\eta(t)|.$$

  We convert the turning rate to degrees per second by dividing by the number of seconds per data step (10 seconds).

- **Turning bias**: this is very similar to turning rate; the only difference is that we omit taking the absolute value of the angles. This means that for a school turning randomly, the turning bias will be zero, but if the school tends to turn more to the left or right, the turning bias will indicate this. Positive values indicate turning to the left, negative values indicate turning to the right.

- **School speed**: the average speed of the center of mass of the school. This is calculated as the average distance between the centers of mass in subsequent data steps, divided by the number of seconds per data step.

2.3 Program design

The simulation program is written in C++ using the Qt framework, version 5.4.1. Qt provides a signal-slot mechanism for communication between objects. This makes it easy to separate the simulation logic from the visualization and outputting of data. For visualization, OpenGL 4.1 is used with shaders written in GLSL.

The program is written to be easily customizable and extensible. This was necessary because the program had to be adapted depending on the results from simulations as the project progressed. Figure 2.6 shows a diagram of the program structure.

The program can roughly be divided into three parts: the model runner, the widget (for visualization) and the statistics reporter (for outputting data). These communicate through signals and slots. Signals are methods that do nothing except

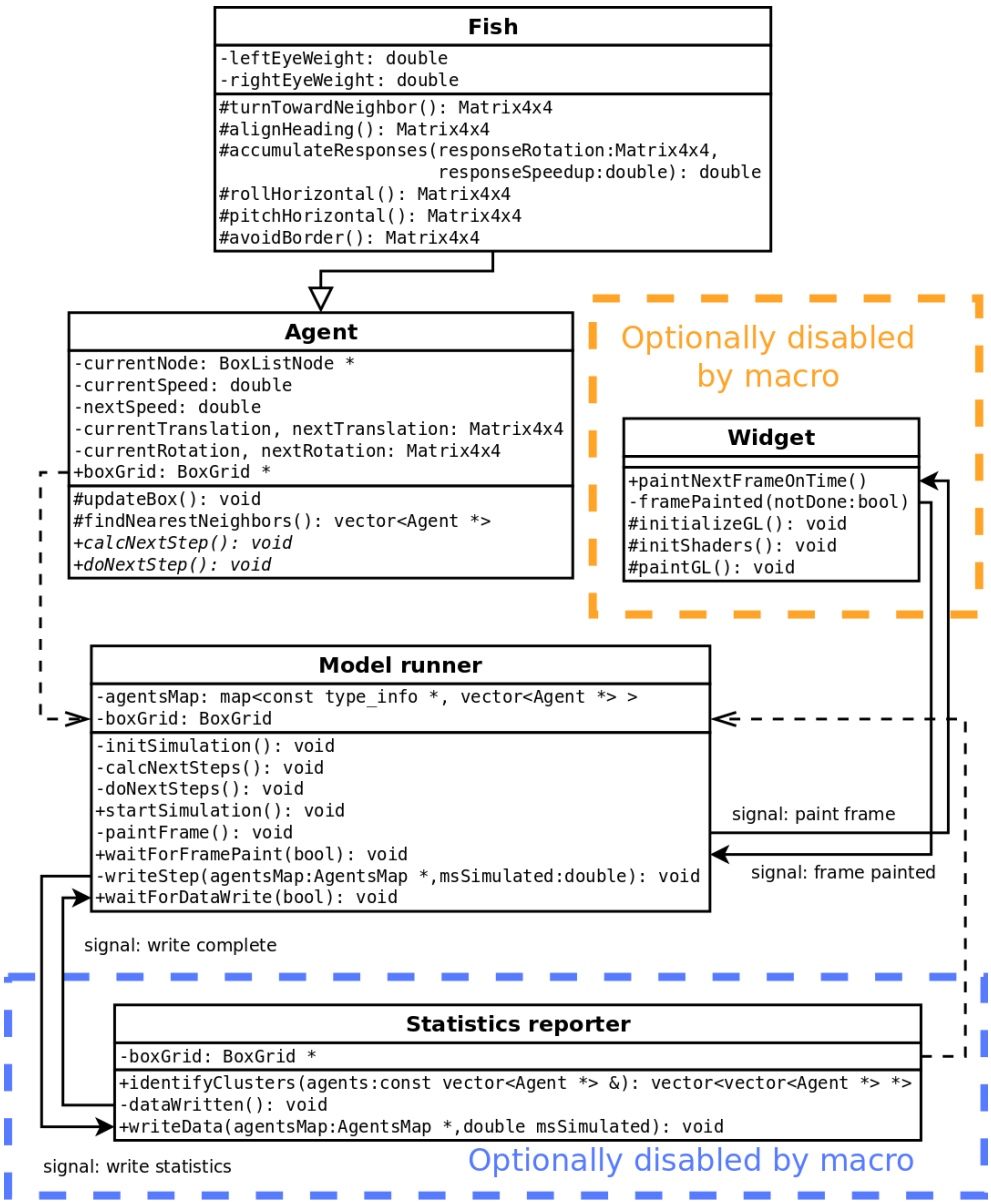

Figure 2.6: Simplified representation of the simulation program.

triggering any slots that are registered to them. Slots are methods that can be registered with signals so that they are executed whenever the signal is called (emitted). Multiple slots can be registered with a single signal, and vice versa. The connections between the different parts of the program are defined in the main function. This way, the model runner, widget and statistics reporter require no knowledge of each other.

- **The model runner**'s main feature is a loop for running the simulation. In each iteration, all agents calculate how to update their state, and subsequently all apply these updates simultaneously. The calculation step is by far the most costly, but since all of its write operations are independent of each other, we can parallelize it. This is easily achieved by adding a `#pragma omp parallel for`-directive before the loop in which the calculations are done. If visualization is enabled, the model runner periodically emits a signal so that the widget paints a frame. If data output is enabled, it periodically emits a signal so that the statistics reporter outputs data to a file. The speed of the simulation can be adjusted. This is necessary because we wish to inspect the schooling behavior at different speeds: real time to see how 'natural' the schooling behavior is, and at higher speeds to quickly inspect the time evolution of the school. When visualization is turned off, the model always runs at maximum speed. Frame rate and data output frequency are both customizable, and the model runner adjusts the number of iterations between emitted signals accordingly. In case of the frame rate, the model emits a signal as soon as a sufficient amount of time has been simulated. The widget responds once it has painted the frame (it mostly waits a bit to control the simulation speed) by emitting a signal. This signal causes the model runner to continue with the next iteration.

  To allow the running of sets of simulations (for exploring a parameter range), the model runner has loops for parameter adjustments around the simulation loop. Once the simulation loop finishes (by whatever criterion), all fish are deleted, a parameter is adjusted and the next simulation is started.

- **The widget** sets up the shaders and maintains several variables related to the visualization, such as the size of the window and the fish that the camera follows. For the actual drawing, it uses a geometry engine member object. The widget also responds to keyboard input so that the user can move the camera, adjust a few settings of the model and exit the program. As mentioned for the model runner, the widget responds to signals from the model by painting a frame when the time is right. Each signal from the model runner contains a reference to the set of agents, which the widget uses for drawing.

- **The statistics reporter** has a very simple job: as soon as it receives a signal from the model runner, it writes data to a file. The signal from the model runner includes a reference to the set of all fish, which the statistics reporter uses to extract data from. Once the write is complete, it emits a signal so that the model runner continues the simulation. In the final version of the program, the statistics reporter periodically calculates which fish are together in clusters. It outputs the indices of all fish in a cluster on a single line, so that each cluster is on a separate line. After that, the speed, position, up and forward vectors of all fish are written to the file.

To make it easy to adjust parameters of the model, the program defines custom namespaces in a file `model_parameters.cpp`. Parameters related to the school

(number of influential neighbors, preferential speed, etc.) are grouped together in a namespace. Parameters of the simulation (frame rate, number of simulations per parameter setting, etc.) are grouped in another namespace. In particular, the simulation namespace contains arrays of parameter values. These arrays are used by the model runner to process an ensemble of simulations. Changing the interpretation of these parameter arrays requires making changes in the model runner. Apart from this, the model parameters file provides a centralized location where all relevant parameter changes can be made, instead of having to search through the source code to find the relevant variables.

Finally, the fish class itself: to facilitate the addition of different kinds of fish to the model (e.g. a predator), the fish class is a subclass of an agent class. The model runner actually maintains a map from type info to vectors of agents, where the type info identifies the kind of agent, and the vector contains all agents of that type. The agent class has a methods `calcNextStep()` to calculate its next state (empty by default), and a method `doNextStep()`, which updates position, translation and information related to neighbor searching. These methods may be overridden by any subclass to customize the behavior of agents. Due to time constraints, the agent class has only one subclass though: the (prey) fish class.

3. Experiments

We performed three sets of experiments: one to investigate the structure of a stable school, and two to investigate the separation of unstable schools. In the experiments where fish were lateralized, we chose to give all fish in the school the same lateralization strength. Only the direction of lateralization varies between fish, this is controlled by varying left- and right-lateralized fractions. This approach may not be realistic, but it makes the analysis of the results much easier.

3.1 Experiment 1: Stable schools

3.1.1 Design

The school is initialized by placing all fish in an axis-aligned bounding box with length-width-height ratios of 3-by-2-by-1. All fish initially face the same way in the length-direction, with their up-vectors also aligned in the height-direction. The choice of the ratio of the initialization volume is somewhat arbitrary, but not very important. Real fish schools show a wide range of dimensions (see e.g. Partridge et al. [1980]), but are mostly longer than wide, and more wide than high. The size of the box in which the school is randomly initialized is set so that a reasonable density is obtained, taking the number of fish and their preferred neighbor distance into account.

An important choice in the model is how a fish determines which neighbors to react to. Simulation studies from the literature have used various different methods for this. Huth and Wissel [1992] for example used priority functions to select nearby neighbors based on their angle and distance with respect to the focal fish. Hemelrijk and Hildenbrandt [2008] let a focal fish respond to all its neighbors within an adaptive radius that changed based on the local density of the focal fish. Parrish et al. [2002] used fixed numbers of nearest neighbors, with 4, 8, 16 or 24 nearest visible neighbors. In the first version of our model, we determined the influential neighbors separately per eye: the focal fish would select the nearest 4 neighbors that were visible to the left eye, and the nearest 4 neighbors that were visible to the right eye. In this way, the focal fish would respond to at most 8 neighbors in total. This approach seemed useful for studying lateralization, and it would enhance group cohesion: a fish on the edge of a school is always 'on the lookout' for neighboring schools. However, testing of this model showed that the school would flatten out very much, quickly ending up as a sheet of only one fish thick. Clearly, this was very unnatural, unwanted behavior. In appendix A the cause of this flattening is discussed, as well as some modelling efforts to avoid it.

In our final model, each fish considers the N nearest neighbors that are visible to it, similar to the model of Parrish et al. [2002]. The parameters of our first set of experiments are listed in table 3.1.

After starting the simulation, every 10 simulated seconds we write the speed, position and orientation of every fish to a file. The simulation may stop based on two criteria: either we have collected the desired amount of data, in which case we are done with the current parameter settings, or the school breaks apart. If the school breaks apart before the desired amount of data has been recorded, we stop the simulation. We keep the collected data, and start a next simulation with the same parameter settings to collect additional data.

Breaking apart of the school is defined as follows: each individual has a cohesion distance, and we consider an individual 'connected' to all other fish within this dis-

time step	0.05 s
world radius	10.000 BL
number of influential neighbors	8
horizontal vision angle per eye	150 °
vertical vision angle	150 °
visual range	15 BL
turning equilibrium distance	2 BL
alignment distance	6 BL
alignment turning angle	15 ° s^{-1}
positional turning angle	100 ° s^{-1}
wall avoidance angle	4 ° s^{-1}
horizontal stabilization	0.20 s^{-1}
fish acceleration	0.20 BL s^{-2}
near distance	0.85 BL
far distance	1.35 BL
maximum noise (yaw)	2 °
maximum noise (pitch)	2 °
preferred speed	2.0 BL s^{-1}

Table 3.1: Parameters used for the stable-school experiment.

tance. Two individuals A and B occupy the same subschool if and only if they are both part of the same connected set of fish, using this definition of connectivity. As soon as there is more than one subschool, the school has broken up. The rationale behind this definition is intuitive; subschools are distinct precisely when there is no cohesive influence between them, so that if they (re)combine, it will be by chance. The data from simulations that end by the school breaking up are still used, we simply combine the data from multiple runs for a single parameter setting.

The following subsections treat three different experiments with the same model, varying different parameters (school size, lateralization strength and lateralized fraction). In all cases, we generate data for 2 hours of simulated schooling time for each parameter setting.

3.1.2 Schoolsize

We first investigate how the structure of the school, as measured by various metrics which we define below, depends on the number of individuals in the school. This is done to gain more insight into the working of the model and for comparison with simulations in the literature. Lateralization is disabled for the school size experiment (i.e., the lateralization strength is set to zero). Full results of the simulations are listed in appendix B. The notable results are treated in the rest of this subsection.

First, a general remark about the results: as we can tell from the graphs for e.g. nearest neighbor distance and school speed (see appendix B), the school of 10 individuals is the odd one out. This is because for very small schools, consensus about direction is easily achieved; the individuals are almost perfectly aligned most of the time. We may think that this is because in our model, each fish looks at 8 neighbors, so that almost every pair of fish is constantly undergoing an alignment interaction. Lowering the number of influential neighbors to 3 does not result in any change though. With 2 influential neighbors the school becomes unstable. It seems that the different behavior of the 10-individual school is because it is small enough for information about direction to spread quickly through the whole school. This quick

spread of information is important for resolving differences in direction that randomly arise in different parts of the school. Structural changes in the 10-fish school occur only occasionaly and cause a sudden change to the swimming direction of the school as a whole. The difference in behavior with larger schools is so big that there is no point in discussing their difference in terms of metrics. In the following paragraphs, we discuss only the size dependence of the larger schools.

Nearest neighbor distance

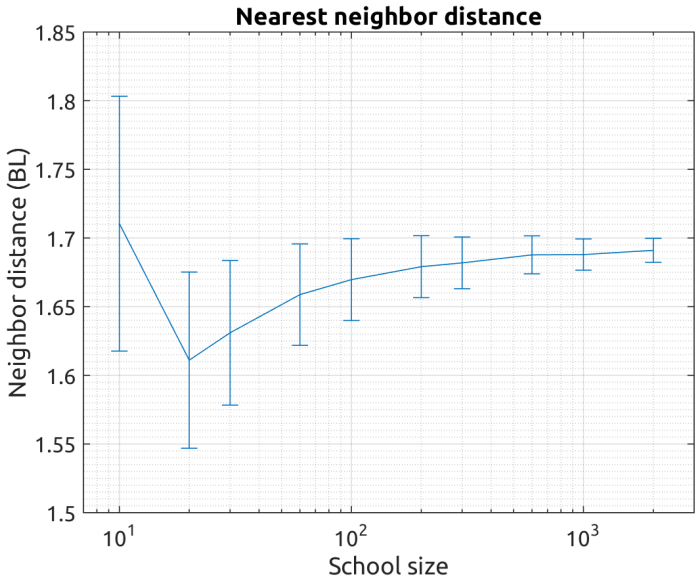

Figure 3.1: Nearest neighbor distance, averaged over all fish and all data steps.

In our model, large schools have higher nearest neighbor distance, see figure 3.1. The increase is especially prominent for schools of up to a hundred individuals. One explanation is that small schools have low nearest neighbor distance because everyone wants to be in the center: individuals near the border of the school exert pressure toward the school, since they are mostly attracted toward their neighbors in the school. In small schools, this is the majority of individuals, leading to a low nearest neighbor distance. Larger schools have relatively more fish inside the school. These fish coordinate with neighbors on all sides, so that cohesions tend to cancel out more or less. Because of this, they tend to have a nearest neighbor distance that is closer to the equilibrium nearest neighbor distance (in our model: 2 bodylengths).

An objection to this could be that the pressure from fish near the border should compress the school until its density is the same everywhere. This is a possibility, but we find it more likely that the physical gas model does not hold in this case; fish that are further into the school are more resilient to repulsion from the border because they also have more attractive neighbors on the side of the border. The alignment interaction also dampens the positional interactions.

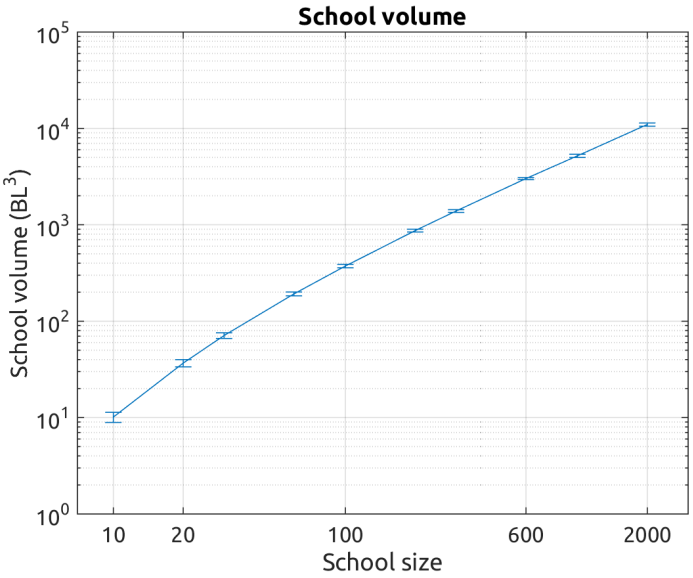

Figure 3.2: School volume, calculated from its alpha shape with $\alpha = 1/4$.

School volume

The volume of the school scales almost linearly with the number of individuals (note the double-logarithmic scale), see figure 3.2. This indicates that density remains mostly equal. From the increasing nearest neighbor distance, we would expect density to decrease with increasing school size. An explanation for this difference could be that nearest neighbor distance is sensitive to inhomogeneity of the school. Smaller schools are apparently less homogeneous, as is confirmed by the lower polarization of small schools.

Polarization

See figure 3.3. Polarization is low for small schools, and increases for school sizes up to 200 individuals. For schools larger than 600 individuals, polarizations seems to slightly decline, and has notably higher variance. This dependence of polarization seems to be caused by two different mechanisms:

- For small schools, a relatively large number of individuals is near the border of the school. Sometimes, such an individual has a random deviation away from the school which leads to it making a full turn before joining the small school at the rear again. These manoeuvers make the polarization much lower.
- In large schools, the 'information' about heading does not travel sufficiently fast to lead to consensus among, say, the front and back of the school. This leads to lower global polarization, even though local polarization can be quite high.

Frontality

See figure 3.4. The high density core is slightly to the front of the school for small schools, and moves to the rear with school size. This is again due to sensitivity

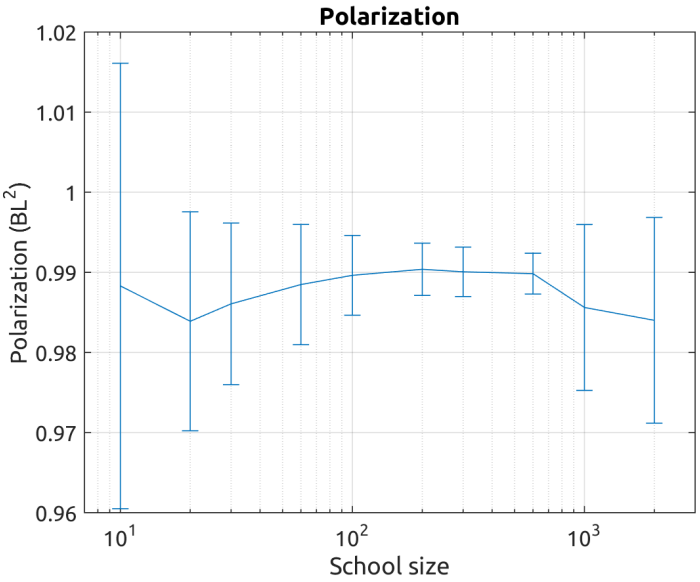

Figure 3.3: Average polarization.

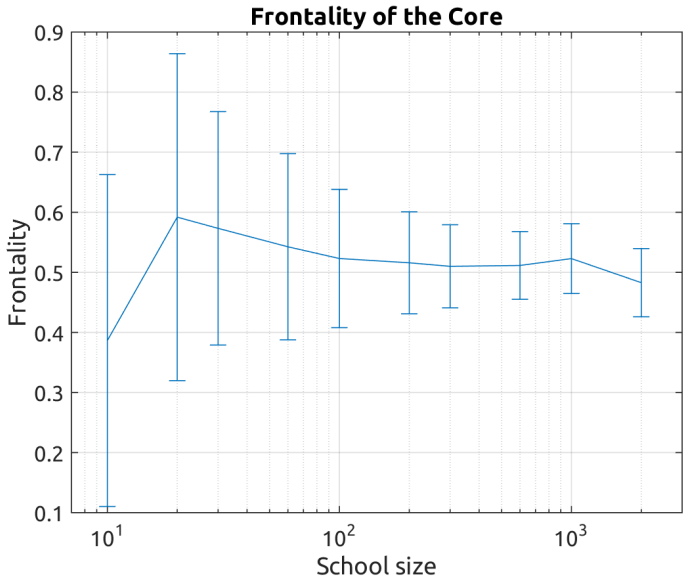

Figure 3.4: Frontality of the core.

to individual contributions: in small schools, the bounding box is more sensitive to individual deviations. The flaking as discussed above not only leads to lower polarization, but also causes the flaking individuals to temporarily end up behind the school. Before they catch up, they stretch the bounding box somewhat to the rear, so that the core is relatively in front. For large schools, frontality becomes 0.5, i.e., the core is situated halfway in the school in the longitudinal direction. In this case, the core has no more meaning, since a school with a random density distribution would give the same result.

Length-over-width

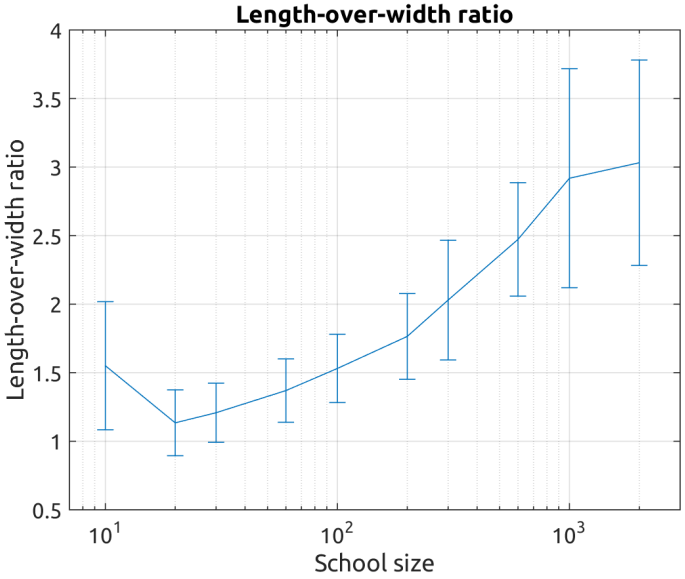

Figure 3.5: Average length-over-width ratio.

The length-over-width ratio clearly increases with school size, see figure 3.5. This has to do with the different 'forces' acting on the sides and front/back of the school. Individuals on the sides of the school constantly exert some pressure toward the school due to cohesion. Individuals at the front and rear only accelerate/decelerate if they are compelled to do so by a neighbor that is in one of their speeding interaction zones (see figure 2.4). The latter hardly constitutes a pressure from the front or back, since all fish happily swim at their preferred speed, which is identical for all fish in the present model.

An explanation for the observed dependence on school size can be that the pressure from the sides propagates into the school. This pressure becomes weaker the further it travels into the school. To understand this, consider an individual outside the school. This individual exerts pressure through its cohesive tendency toward the school. Its neighbor, slightly in the school, responds to this pressure by pushing back (it has some inertia, and the repulsive interaction works both ways of course), but is also repelled to move further into the school. In this way, the 'pressure' exerted from the sides becomes weaker the further into the school it travels. Nevertheless, if there were no opposing pressure (namely, the pressure from the opposite side of the school) eventually all individuals would turn sideways. This of course does not occur because

an equilibrium between these pressures is established. This happens at the center of the school, where individuals have neighbors pushing from both sides equally.

If the school is very narrow (say, 4 BL), this pressure is quite high, leading to dynamic zigzag movements of individuals. The gaps that are inevitably caused by this are filled by neighbors in front or at the back, by changing their speed. If the school is too broad, the lateral pressures on individuals in the center are very low. This means they are quite free to optimize their nearest neighbor distance so that are they are neither attracted nor repelled by their neighbors. A broad school also means that alignment information takes longer to travel laterally through the school; If we start with a broad school, the sides of the school both move toward the center through the pressure of fish at the sides. When these two groups collide at the center, this causes a sudden increase in density, which leads to individuals accelerating/decelerating so that the school becomes more longitudinal. It therefore seems that neither very narrow nor very broad schools can be stable, and they tend toward some (possibly broad range of) equilibrium width. Note in particular that the above considerations that lead to a certain school width are independent of the number of individuals in the school. Our reasoning therefore leads us to expect that width is more alike for schools of different sizes than length or height. If this is the case, then larger school must necessarily become longer and/or higher, or have a higher density. Our model shows that density does not increase (the volume increases linearly with school size, see figure 3.2) and instead both the length and the height of the school increase.

Width-over-height

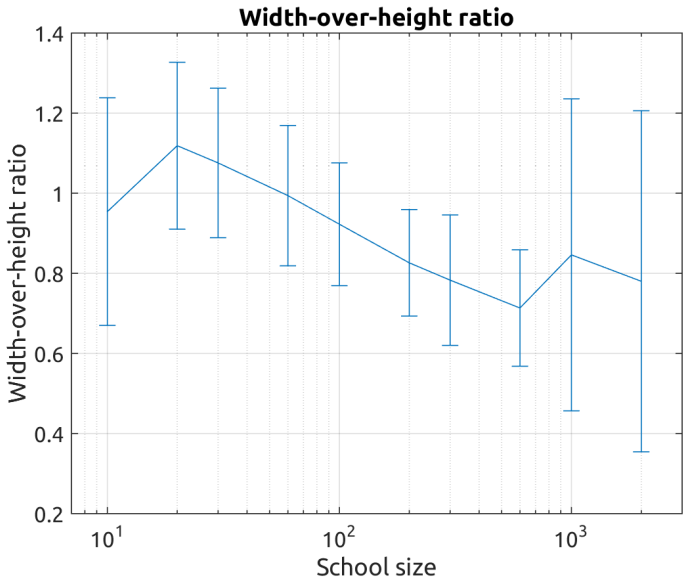

Figure 3.6: Average width-over-height ratio.

The width-over-height ratio decreases with school size, see figure 3.6. In part this is explained by the previous paragraph, but there is a supplimentary explanation: Large schools deform, and tend to become amorphous. A vertical, amorphous extension of the school can be formed through repulsive interactions and noise. Since pitch is stabilized, vertical turns are not as strong, so that the relative importance

of alignment increases in this direction. Because of this, 'information' about vertical position travels quite slowly through the school. Horizontal cohesion is unimpeded by pitch stabilization, so that fish easily make turns in the horizontal direction, and information travels fast in this direction. This means that the vertical extension of the school is quite rigid, while the plastic, horizontal structure can easily correct any deformations that occur.

Turning rate

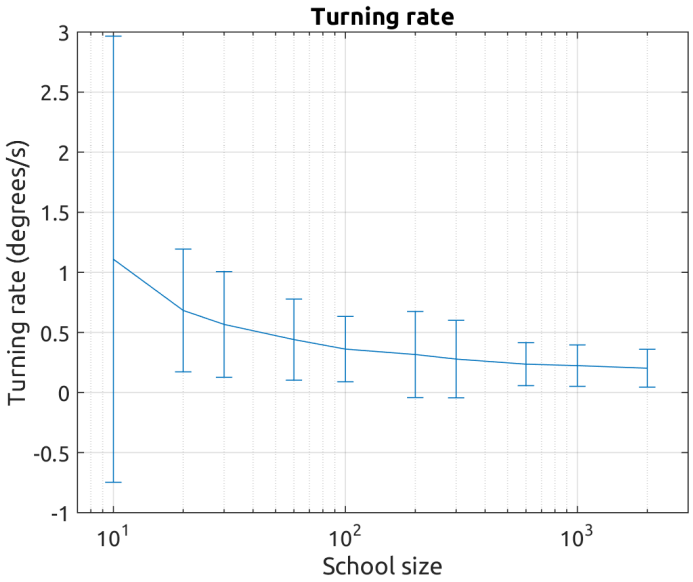

Figure 3.7: Average turning rate of the school.

The turning rate of the school decreases for increasing school size, see figure 3.7. This is what we would intuitively expect; small schools are more sensitive to the random movements of individual fish that cause them to turn. The anomaly of 10 fish is in line with our previous description of it; the school swims very much aligned for moderately long time periods but makes sudden turns in between. These sudden turns lead to the high turning rate, and the contrast between aligned schooling and sudden turns results in the high standard deviation.

Speed

Large schools are in general faster than small schools, see figure 3.8. There are multiple possible explanations for this: the first explanation was also given by Kunz and Hemelrijk [2003], and is based on the observation that smaller schools are less polarized. This means that in small schools, fish zigzag more so that their effective forward movement is smaller. Secondly, we note that the school speed is lower than the individual preferred speed. This may mean that decelerating speeding interactions are more frequent than accelerating ones. Net deceleration occurs if a fish approaches a neighbor in front of it in the blind angle of that neighbor. The focal fish will decelerate without causing an equal amount of acceleration in the neighbor in front, leading to a net deceleration of the school. Such decelerating interactions are likely more frequent in schools with lower nearest neighbor distance. This is confirmed

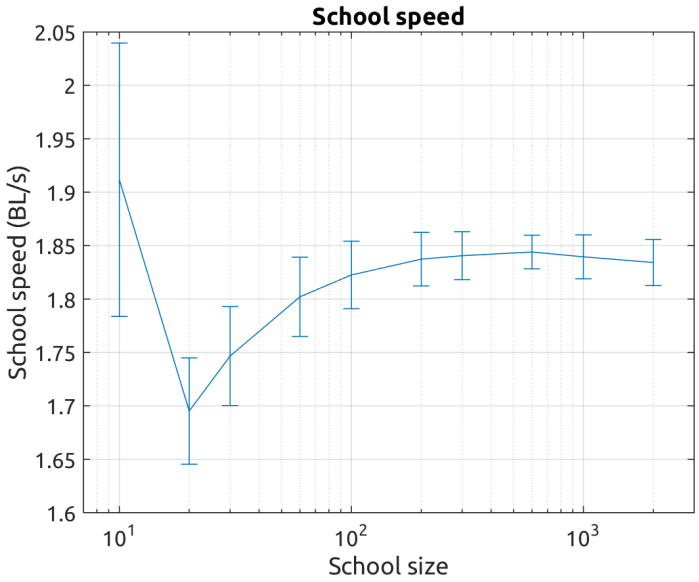

Figure 3.8: Average speed of the school.

by the nearest neighbor distance that we found, which has the same dependence on school size as the school speed (see figures 3.1 and 3.8).

An additional influence is that smaller schools have a higher turning rate, a correlation that was also found by Kunz and Hemelrijk [2003]. Since our data steps are recorded only every 10 seconds, our speed metric 'cuts corners' for turning schools.

3.1.3 Lateralization strength

For this experiment, we set the school size to 200 with equal lateralization fractions (half of the fish are left-lateralized, the other half is right-lateralized) and determine the range of lateralization strengths for which the school remains stable. In the graphs below, lateralization strength is defined so that a lateralization strength of zero corresponds to no lateralization - responses are equally strong for neighbors on the left and neighbors on the right. A lateralization strength of one means that the responses are determined by neighbors on one side, completely ignoring the neighbors on the other side. Full results are again listed in appendix B, and the most notable results are treated in the rest of this subsection. The most important thing to note about this experiment is that the left and right lateralized individuals assort themselves into (overlapping) groups. The right lateralized group tends to be on the left side of the school, and the left lateralized group tends to be on the right. This means that in our model, the lateralized fish are located in the school in such a way that they use their 'strong' eye to look toward the (center of the) school.

Nearest neighbor distance

Nearest neighbor distance increases with lateralization strength, see figure 3.9. This is because left-lateralized fish tend to turn to the right and vice versa for right-lateralized fish. The reason for this will be discussed in section 3.1.4. With individual turning biases, the two lateralized fractions assort themselves into left and right groups that

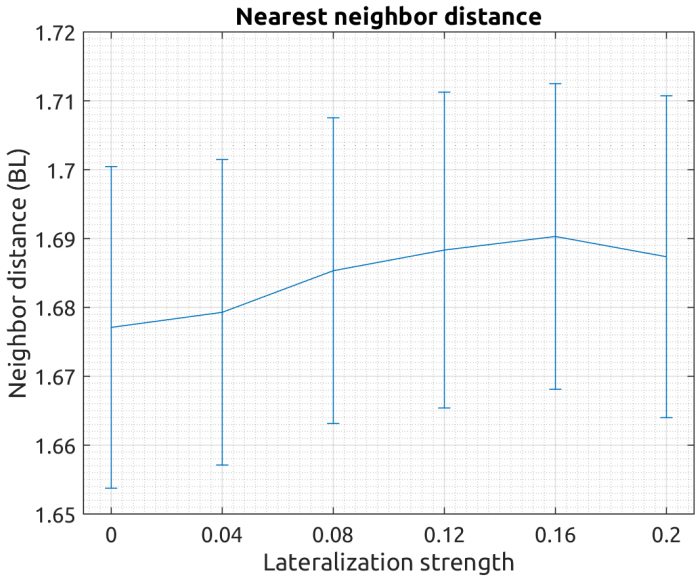

Figure 3.9: Nearest neighbor distance.

tend to pull the school apart (see section 3.1.3). This leads to higher nearest neighbor distance in the school.

Interestingly, the nearest neighbor dependence on lateralization strength has a sigmoid shape. For weak lateralization, the slow increase in nearest neighbor distance may be because the lateralization influence simply needs to overcome the stochastic interactions in the school. As lateralization approaches the limit of stable schooling behavior, nearest neighbor distance does not increase as fast anymore. This may be because the groups are already separated so well that there is little more separation to gain.

Volume

The volume of the school has roughly the same dependence as the nearest neighbor distance, see figure 3.10. The school volume is comparatively low for strong lateralization. This may be because for strong individual lateralization, the school becomes much wider (see width-over-height). As surface area increases, the volume of the school decreases according to our measure: the alpha shape namely encloses encloses the school tightly, so fish near the border 'contribute' less volume than those inside the school. Another factor is that polarization is low for a lateralization strength of 0.2 (see figure B.3c), so that neighbor distance is less homogeneous, leading to a lower nearest neighbor distance.

Frontality

Frontality of the core increases with lateralization strength, see figure 3.11. This might be due to an increase in flaking of frontmost individuals; since these have a preference for cohesion on one side, they are more easily compelled by neighbors behind them to turn sideways and wrap around the school. As explained for frontality of the experiment with varying school sizes, this leads to higher frontality. However no significant increase in flaking was observed in the schooling behavior, probably because

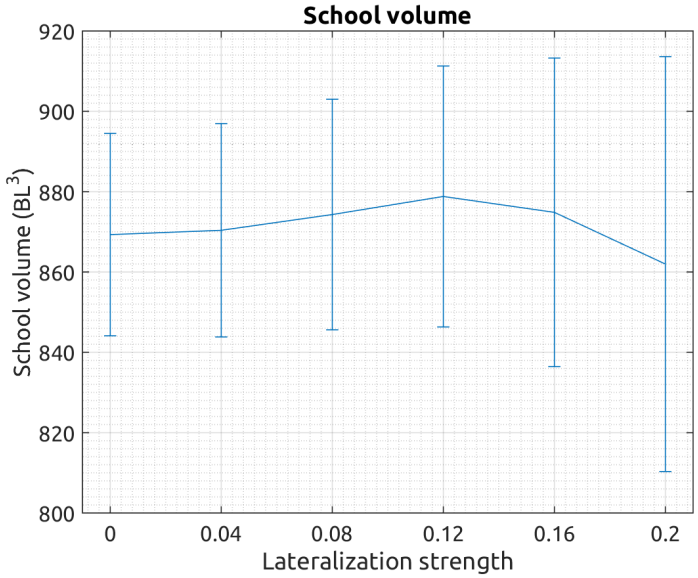

Figure 3.10: Volume of the alpha shape with $\alpha = 1/4$ around the school.

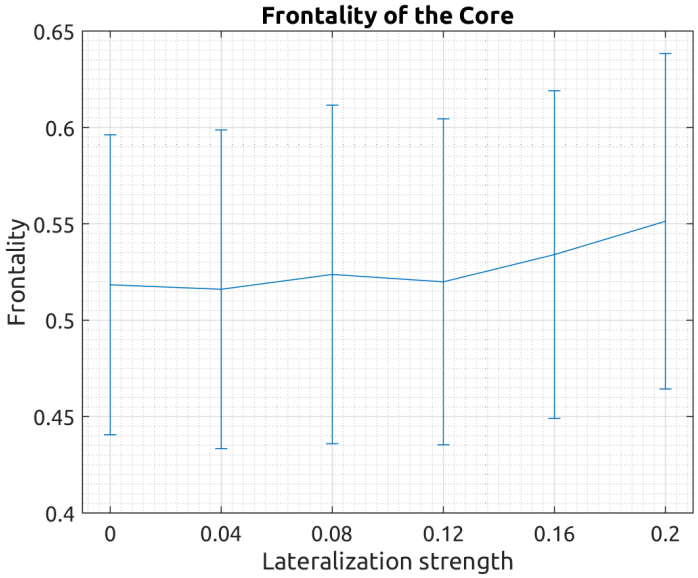

Figure 3.11: Frontality of the core.

the lateralized individuals look toward the school with their strong eye, rather than away from it. By visual inspection, the difference in density appears to be mostly due to a low density tail. This may be because the tail frequently moves in a slightly different direction than the front of the school, simply through stochastic effects. Of course, it mostly follows the head because of cohesion, but it takes a longer path in total. This causes it to spread out somewhat, so that density in the tail is sometimes lower than in the rest of the school. With stronger lateralization, the stochastic tendency of the tail to deviate in direction from the head increases, so that frontality of the high density core increases.

Length-over-width

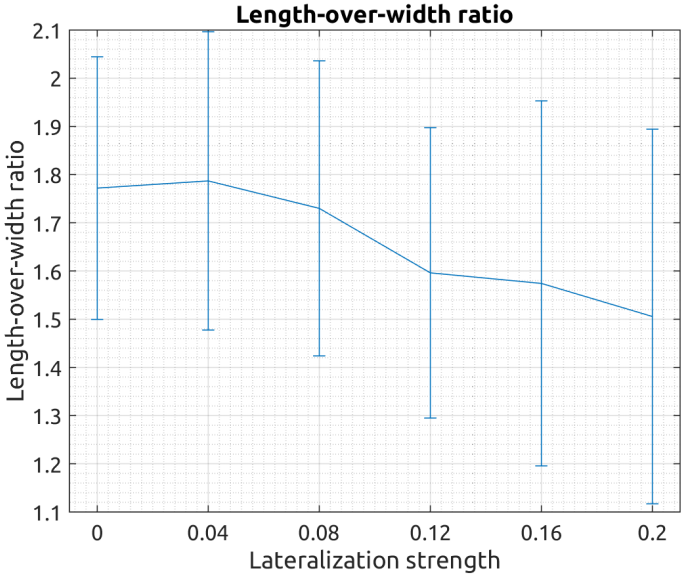

Figure 3.12: Average length-over-width ratio

Strong lateralization leads to wide schools (with a 50/50 distribution of left and right lateralized individuals), so that the length-over-width ratio decreases, see figure 3.12. This is clearly because of the sideways assortment of lateralization types as explained for nearest neighbor distance.

Width-over-height

See figure 3.13. The width-over-height ratio increases with lateralization strength, this is due to an increase in width of the school. The reason behind this is explained for nearest neighbor distance.

Left/right separation

The separation of left and right lateralized individuals has been the explanation for most of the above metrics. Figure 3.14 shows that left/right separation increases with lateralization strength. Positive left/right separation means that left-lateralized fish end up on the right side of the school, and vice versa for right-lateralized fish. Hence, the fish position themselves in such a way that they look toward the group of opposite

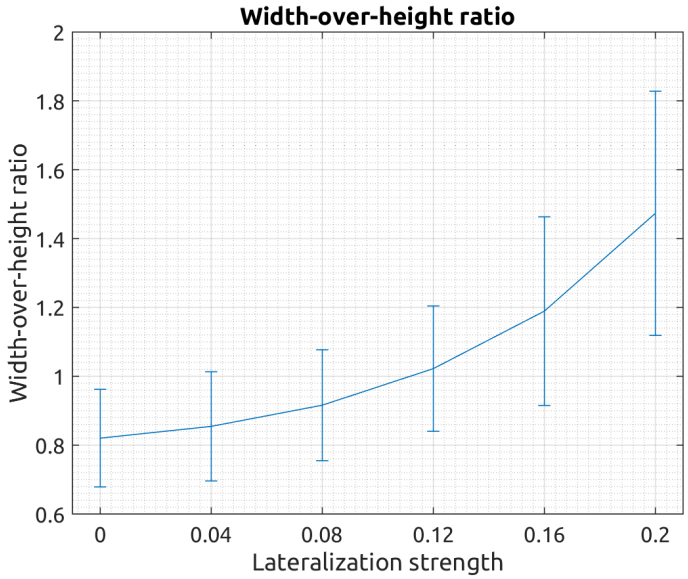

Figure 3.13: Average width-over-height ratio.

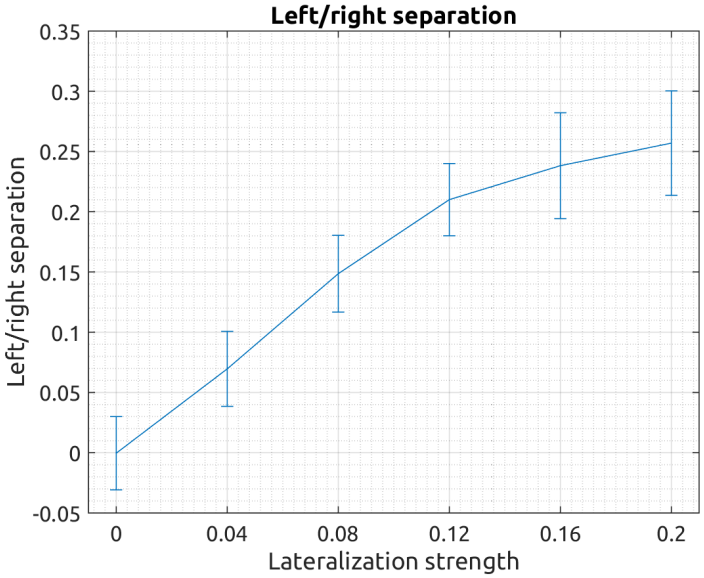

Figure 3.14: Left/right separation.

lateralization with their 'strong' eye. It therefore seems that repulsive interactions outweigh cohesive ones in determining on which side a fish ends up. This hypothesis is strengthened by simulations with an adaptation of the model that used a horizontal cohesion bias (as discussed in appendix A). With this horizontal cohesion bias, the two lateralization types assorted themselves in groups as well, *but on opposite sides*, i.e., looking at each other with their weak eye. The two groups formed an oscillatory movement, coming together and moving away from each other again. This dynamic seems to be dominated by cohesion. For the coming together this is obvious, but the moving apart may require an explanation: rather than turning apart through separation, the two groups try to turn in the opposite direction autonomously. This is because their members feel higher cohesion to their neighbors toward the border (that have the same lateralization type) than the other way around.

Turning rate

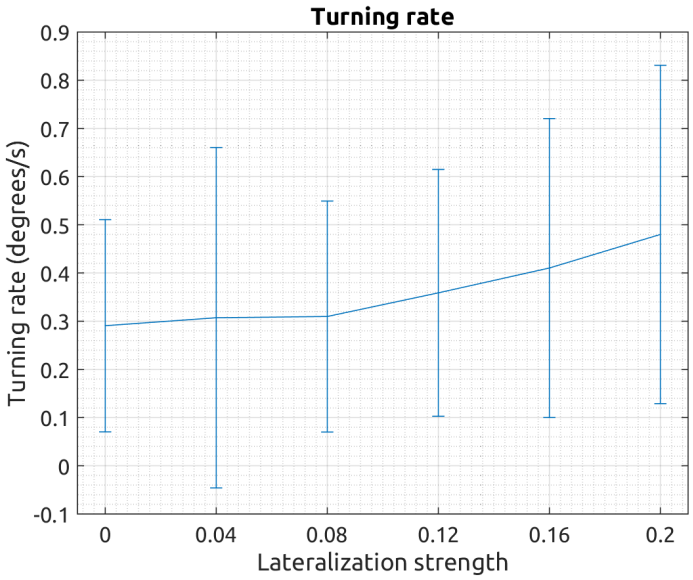

Figure 3.15: Turning rate.

The turning rate of the school increases somewhat for stronger individual lateralization, see figure 3.15. We may explain this by realizing that the frontmost individuals in the school mostly determine the turning direction. The ratios of left- and right-lateralized fish in the front randomly varies. If one of the types has a majority in the front, the school will turn accordingly. Once the school is turning sufficiently fast, the sorting of the school becomes important: either the left or the right half will be swimming along the inner curve during the turn, and get ahead in this way. This positively reinforces the turning tendency, until either the balance is restored again through random movements, or the tail, which mostly consists of one lateralization type, breaks away from the front half.

School speed

School speed initially increases with lateralization strength and decreases only for the strongest lateralization strength of 0.2, see figure 3.16. As in the school size

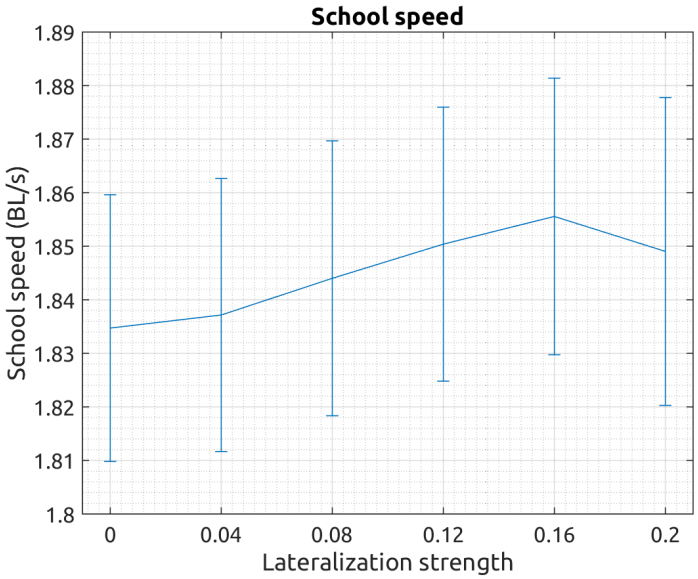

Figure 3.16: School speed.

experiment, this characteristic closely resembles that of nearest neighbor distance, and the explanation we gave for school size dependence is also applicable here. An additional explanation for the decrease at the lateralization strength of 0.2 is that the polarization of the school decreases here; more individual zigzagging results in a lower school speed.

3.1.4 Lateralized fraction

In this experiment, we fix the number of individuals again at 200, and set the lateralization strength to 0.16. This means that left-lateralized individuals will respond more strongly to neighbors on their left, and right-lateralized individuals more strongly to neighbors on their right. We then vary the (left-)lateralized fraction.

Nearest neighbor distance

Nearest neighbor distance decreases with increasingly uneven fractions, see figure 3.17. This is can be explained by the same mechanism that explains the increase with lateralization strength. For equal fractions, the lateralization types form two balanced groups of individuals on either side of the school. As these fractions become more unequal, the smaller fraction loses volume and is absorbed into the larger group.

Volume

The school volume is fairly constant for equal fractions and suddenly increases at 0.8, see figure 3.18. This seems to contradict nearest neighbor distance, which is lower for strongly unequal fractions, implying higher density and thus lower volume. We have two explanations for this:

1. The variation in neighbor distance may increase for more unequal fractions. This could decrease nearest neighbor distance without affecting average density of

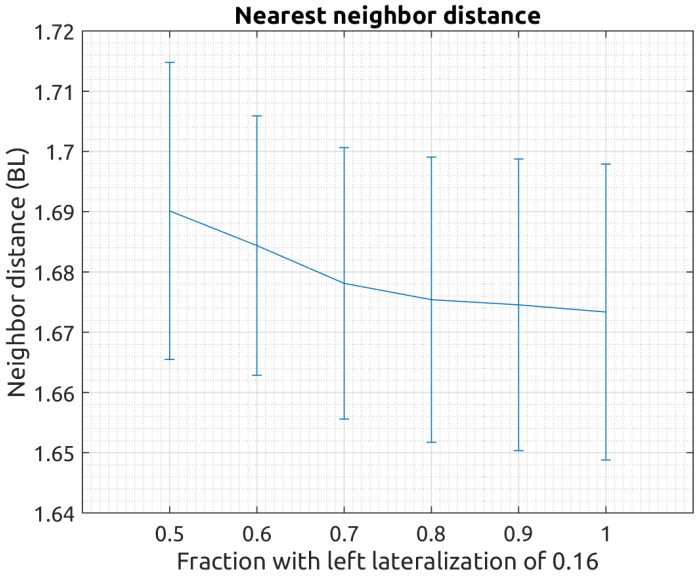

Figure 3.17: Average nearest neighbor distance.

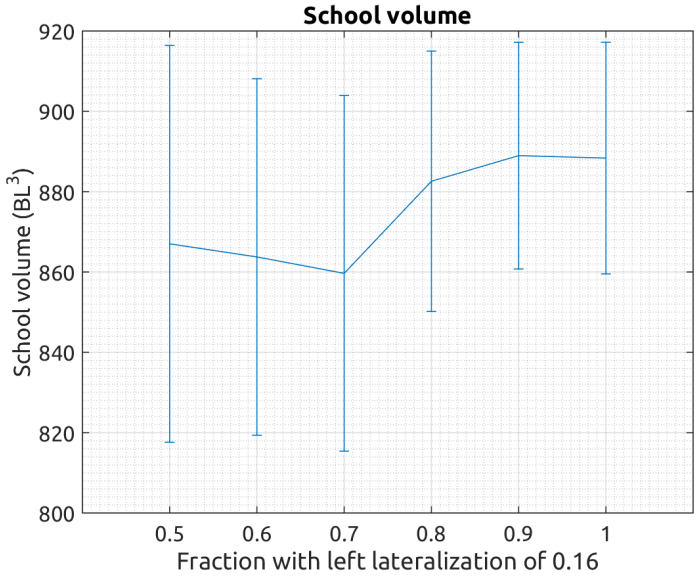

Figure 3.18: Volume of the alpha shape with $\alpha = 1/4$ around the school.

the school. The lower polarization for stronger lateralization appears consistent with this. The slight increase in polarization for very strong lateralization may have a different cause, see section 3.1.4. Ideally, we would have calculated the variation in neighbor distance from our data, but time did not allow for this.

2. The volume metric is sensitive to surface area - a relatively high surface area results in a lower volume metric. This sensitivity was already discussed in the results for lateralization strength. Looking at the length-over-width and width-over-height we see that the school is most spherical for strongly uneven fractions. For a majority fraction larger than 0.7, length-over-width plummets, causing a sharp increase in the volume metric.

Frontality

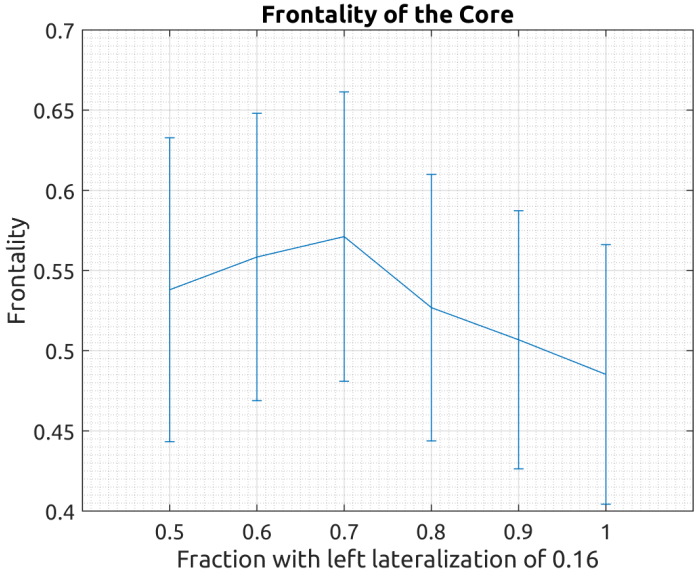

Figure 3.19: Frontality of the core.

Surprisingly, frontality attains its maximum for a moderate majority of one lateralization type (0.7), see figure 3.19. This could be explained as follows: the school turns in circles for uneven fractions (see fig 3.28b). The individuals of majority-type lateralization take the inner curve (which is of course shorter) so that they end up primarily in front. Some majority-type individuals do end up in the tail, where the mingle with the minority-type individuals. Since the tail has a higher fraction of minority-type individuals, its turning tendency is not as strong, and so it tends to describe a larger circle than the front, thereby stretching out. This alone would lead to larger nearest neighbor distance in the tail. The effect may be strengthened by the fact that there are more equal fractions of lateralization in the tail. As we saw in this experiment, nearest neighbor distance is highest for equal fractions of lateralization.

For only one type of lateralization, the mixed tail can obviously not form, and for equal fractions, no turning occurs. Both are necessary to increase frontality. To verify the above explanation, we calculated the frontality of the left- and right-lateralized subgroups separately (except with respect to the global center of mass, rather than

the center of the bounding box). The results are shown in figure 3.20. We see that the majority type indeed ends up in front, relative to the minority.

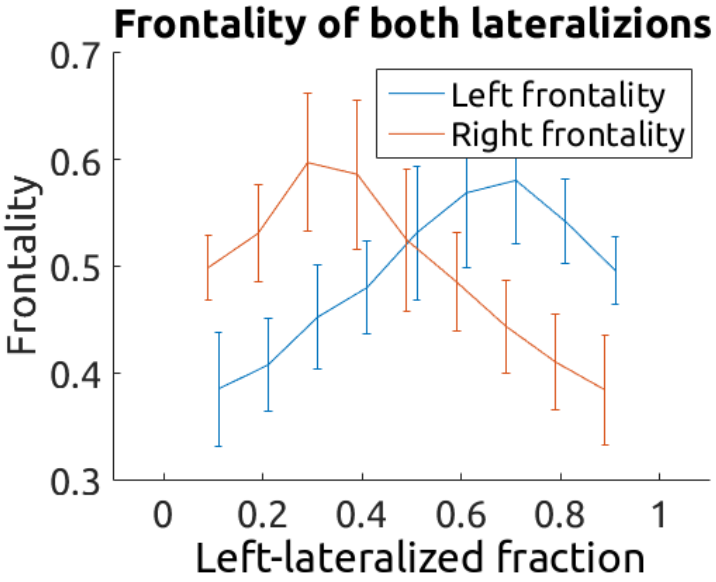

Figure 3.20: Frontality of the subgroups with left and right lateralization.

Polarization

Polarization is highest for equal fractions of lateralization and attains a minimum for intermediate population-level lateralization, with a majority fraction of around 70%. This dependency can be explained by the turning behavior of the school which causes a mixed tail to form. We explained this behavior in the previous subsection. There are two aspects to explaining the dependency of the polarization:

1. For equal fractions of left- and right-lateralized fish, nearest neighbor distance is high. Because of this, individuals spend less time avoiding collisions, and are therefore able to better align their movement directions. This increases polarization.

2. In longer schools, a greater difference may form between the movement direction of individuals in the front and those in the back of the school; if the front turns, it takes some time for the back to also turn. This effect is even stronger in the present case because of the turning bias of the school: the front constantly turns in the same direction, causing a constant difference in movement direction between the front and the back. Since the school is longest for intermediate population-level lateralization, the effect will be strongest here. Our results indeed show that polarization is minimal for such intermediate fractions.

For very unequal fractions, polarization is slightly higher than the minimum, but seems constant. This may be because opposing influences on polarization are balanced here: polarization tends to decrease due to the increasing turning rate of the school (figure 3.25) and slightly decreasing nearest neighbor distance (figure 3.17). On the other hand, the shortening of the school (figure 3.22) would increase polarization.

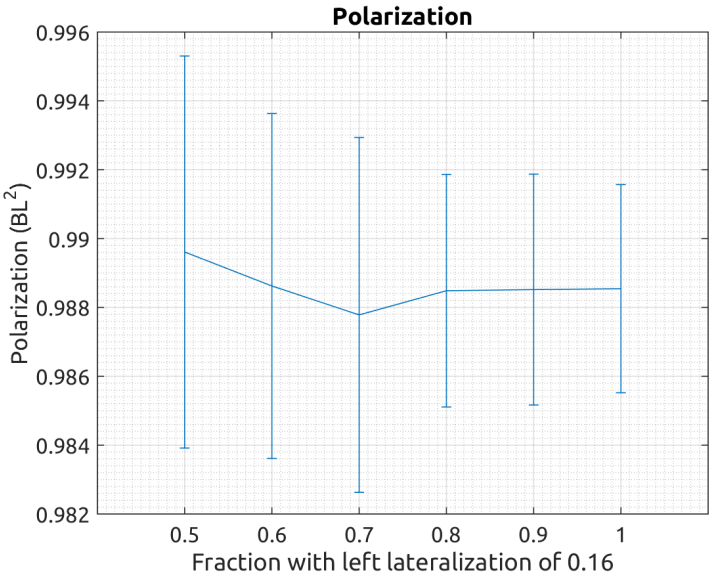

Figure 3.21: Polarization.

Length-over-width

See figure 3.22. In this experiment, the behavior of length-over-width is strikingly similar to that of frontality; it is maximized by a moderate majority fraction of 0.7. The explanation is also the same: with intermediate fractions, a tail of mixed lateralizations is formed. This tail swims in larger circles and thereby stretches out, making the school longer.

Width-over-height

Width-over-height of the school decreases with increasingly unequal fractions, see figure 3.23. This is for the same reason as the increase in nearest neighbor distance: for equal fractions, the lateralization types form two balanced groups of individuals on either side of the school that effectively repel each other. As the fractions become more unequal, the majority group absorbs the minority as we approach the single-fraction case.

Left/right separation

Left/right separation becomes weaker as the fractions become more unequal (note the negative values on the y-axis), see figure 3.24. The reason is the same as described for nearest neighbor distance. Additionally, as the fractions become more unequal, the majority fraction increasingly determines the center of mass of the school as a whole, so it is not surprising that the center of mass of the majority fraction gets relatively closer to it.

Turning rate and bias

Turning rate of the whole school strongly increases, the more unequal the fractions are. See figures 3.25 and 3.26. Comparing the turning rate to turning bias shows that virtually all turning is due to the bias. The school has a strong tendency to

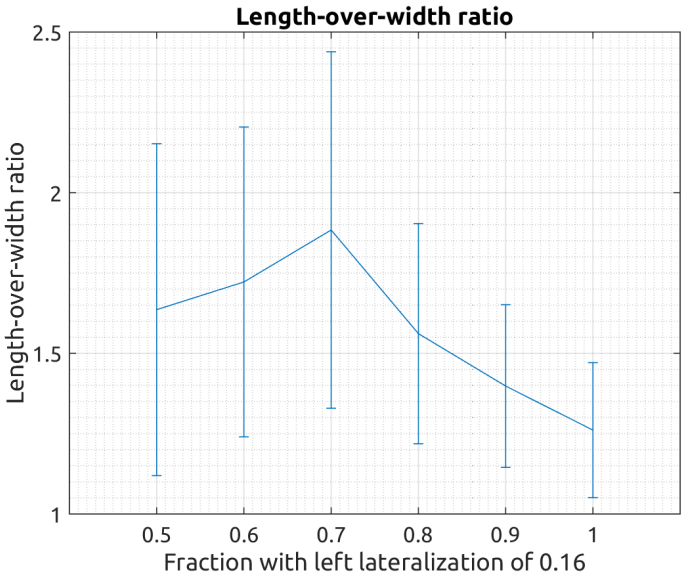

Figure 3.22: Average length-over-width ratio.

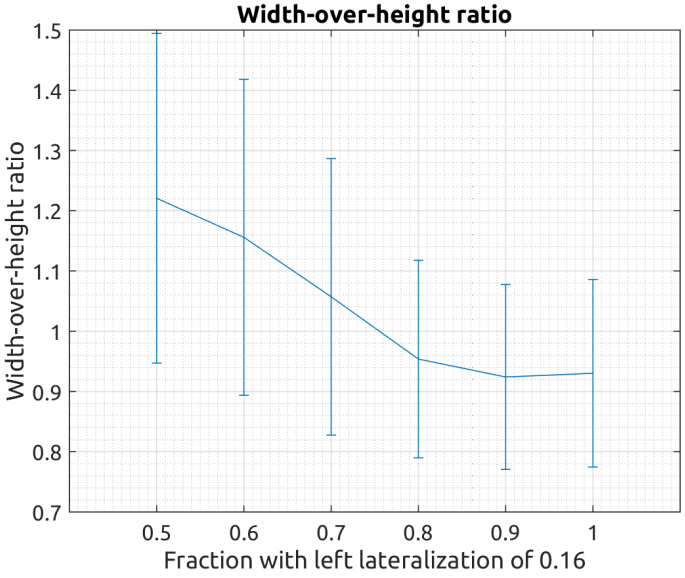

Figure 3.23: Average width-over-height ratio.

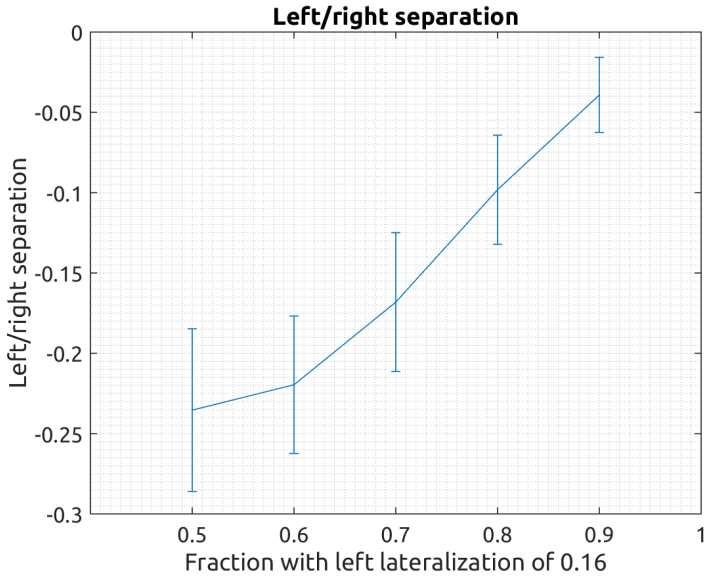

Figure 3.24: Left/right separation.

turn toward the side of the weaker eyes. This can be explained by considering two left-lateralized fish (i.e., fish with 'strong' left eyes). When these fish get close to each other, the fish on the left only weakly responds to the presence of its neighbor by turning to the left, while the fish on the right turns to the right more strongly. Such a repulsive interaction among individuals of the same lateralization therefore leads to a net turning to the side of the weak eyes. One might argue that this asymmetry works the opposite way for cohesive interactions. This is true, but in our model the school is apparently dense (or inhomogeneous) enough to make repulsion the dominant interaction for determining the turning direction.

School speed

School speed strongly decreases for more unequal lateralized fractions, see figure 3.27. As in our experiments with school size and individual lateralization strength, school speed follows the dependence of nearest neighbor distance. The explanation for this was given for school size. In addition, in this set of simulations, the turning of the school may contribute to a lower school speed; since we only record data points every 10 seconds, we do not measure the full path length of the school, but cut some corners for this measure. Stronger turning will therefore reduce the school speed metric, and this is indeed what we observe (compare figures 3.27 and 3.26).

3.1.5 School trajectories

To see how schools moved over the course of the simulation, we plotted their (x, z) position over time (a top-down view of the path traversed). This is important for validating the correctness of our simulation program; in previous sets of simulations, long-term (10 minutes) directional biases were revealed. Figure 3.28 shows the trajectories of schools with various school sizes (3.28a) and various lateralized fractions (3.28b) for the stable schools experiment.

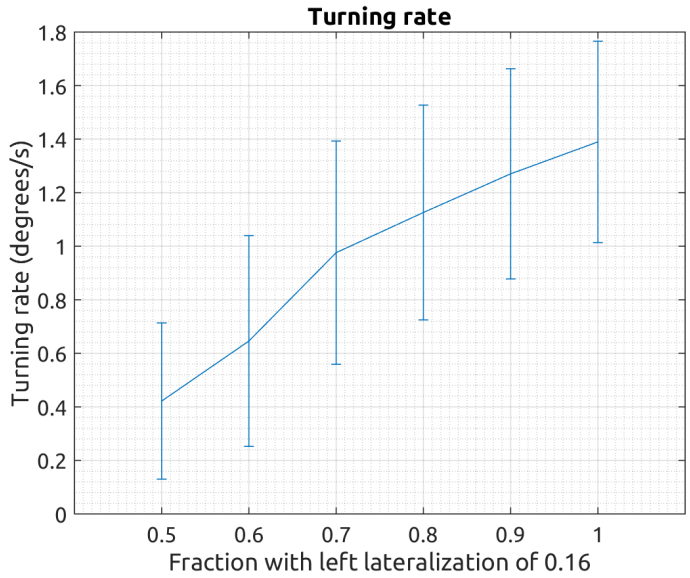

Figure 3.25: Average turning rate of the school.

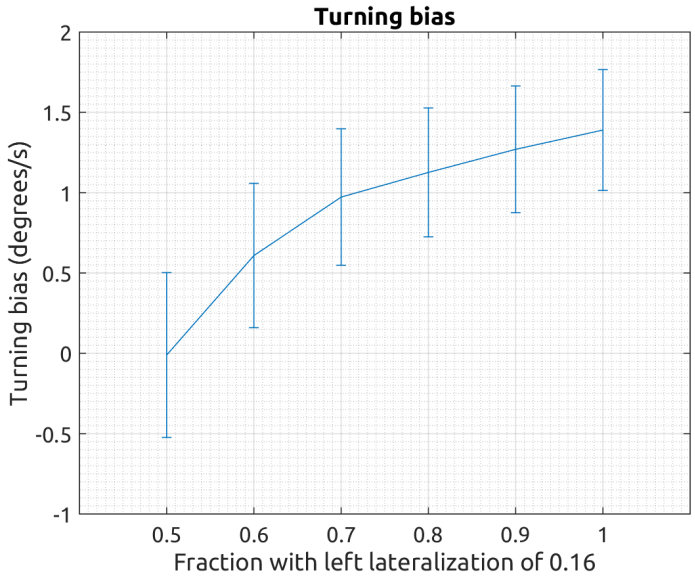

Figure 3.26: Turning bias.

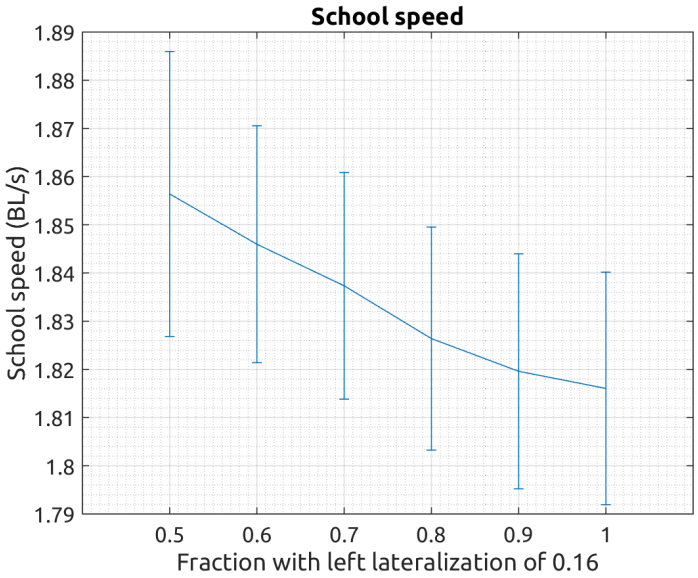

Figure 3.27: School speed.

3.2 Experiment 2: Unstable schools

In experiment 1, parameters were calibrated in such a way that the school stayed together, and we focussed on the properties of these stable schools. We now investigate how lateralization influences unstable schools. Instead of resetting the school once it falls apart, we let each instance run for a fixed time, regardless of the school splitting up. In this experiment we look in particular at school size, and whether individuals of the minority or majority type of lateralization end up in schools of different sizes.

3.2.1 Design

To create an unstable school, we adapted the model of experiment 1 by changing two parameters:

1. Instead of 8 neighbors, each fish interacts with 6 neighbors.
2. The alignment angle has been reduced from $15°s^{-1}$ to $5°s^{-1}$.

We initialize the experiment with 300 individuals. Lateralization strength ranges from 0 to 0.28 in steps of 0.04 and we perform 20 runs for each setting. Each run lasts 890 (simulated) seconds. The school does split up much sooner, but it takes more time for the subschools to disperse, without any chance recombinations occurring any more (which drastically change the measured school sizes).

3.2.2 Influence of lateralization strength on subschool size

We process only the final data step of each simulation instance. For each individual, we determine how large its subschool is. Subschools are determined in the same way in which splitting of the school was detected in the previous experiment. We do this separately for the 75 left-lateralized individuals and for the 225 right-lateralized individuals.

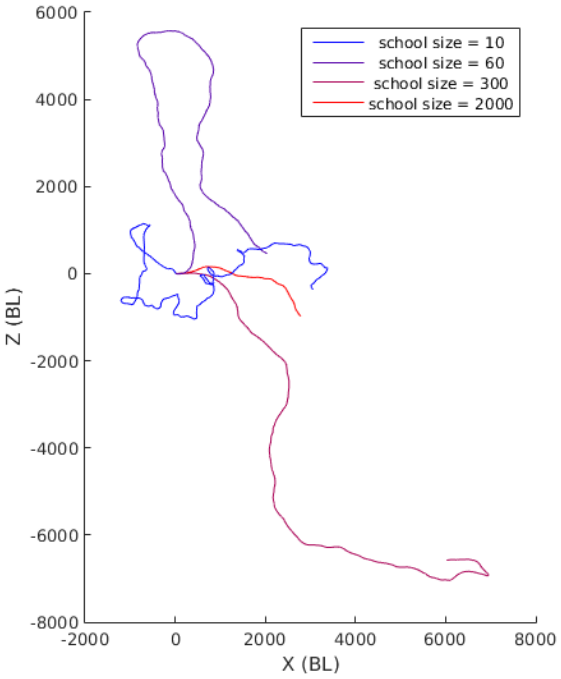

(a) Trajectories of unlateralized schools using 8 influential neighbors for different school sizes.

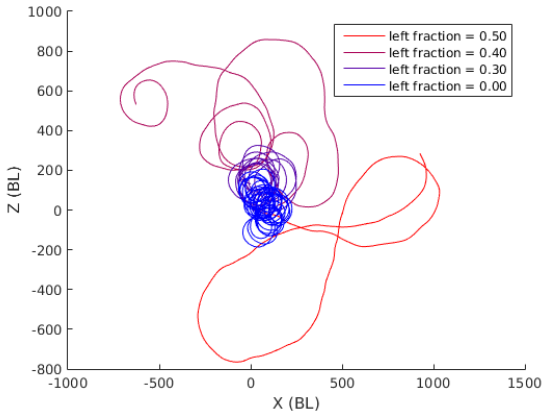

(b) Trajectories of schools of 200 individuals with lateralization strength set to 0.16 for various fractions.

Figure 3.28: A top-down view of the trajectories of schools in the stable schools experiment. Distances are in body lengths.

For each group, we calculate the mean subschool size. Finally, of all these mean subschool sizes, we take the mean and the standard deviation for the left and right groups. The results are plotted in figure 3.29.

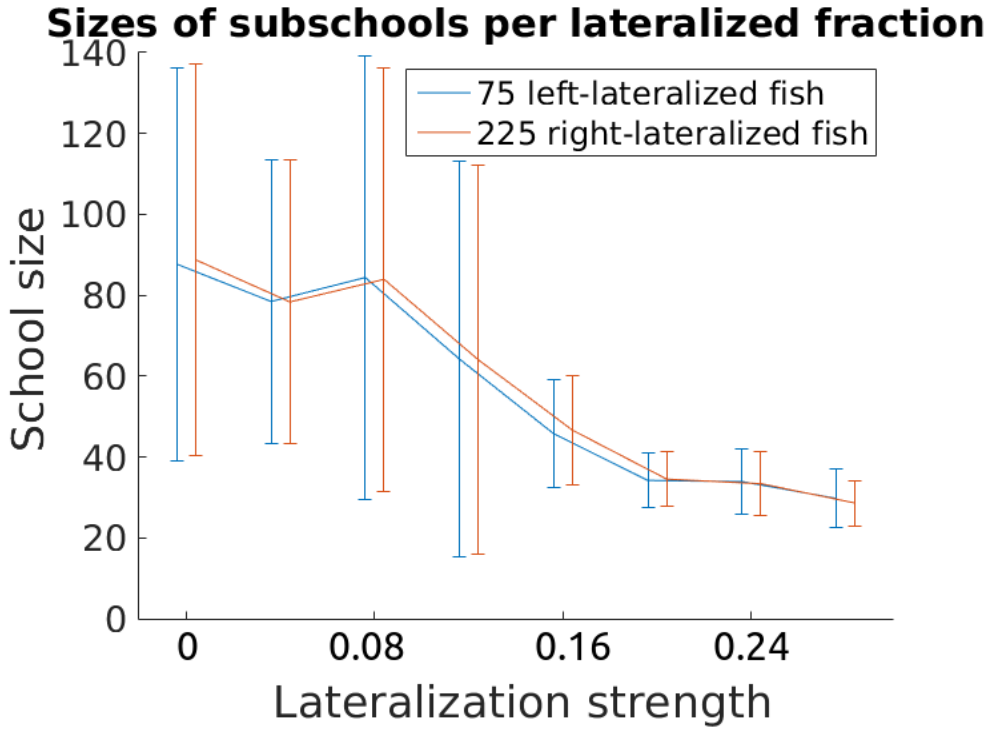

Figure 3.29: Subschool sizes for minority and majority type lateralization, as a function of lateralization strength.

From the figure, we can tell two things:

1. Stronger lateralization results in significantly smaller schools. There is also much less variation in school size for strong lateralization. This is because large schools often split into subschools of unequal size. The smaller subschool is often small enough to be stable, but the larger subschool will probably split again. For low lateralization strength, the larger subschool is more stable and thus the variation in size is preserved. If we were to assign a probability of breaking up to a school, this would be increasing with school size and with lateralization strength. Experiment 3 further explores this dependence.

2. The subschools seem to be well-mixed; the different lateralization types have the same expected subschool size. This is probably because the time needed for the school to assort itself by lateralization type is longer than the time it takes before the school breaks apart. This means that at the time when the school breaks apart, it is still well-mixed, and so the resulting subschools are also well-mixed.

Although the mean subschool size is the same, there might still be some difference in the distribution of subschool size. Minority-type fish could for example have a higher relative occurrence in both small and large subschools, with majority-type fish occurring more often in schools of moderate size. To test this possibility, we create

histograms of subschool sizes for two lateralizations: 0 and 0.2. The results are shown in figure 3.30. We see that, as expected, subschools are well-mixed at all sizes.

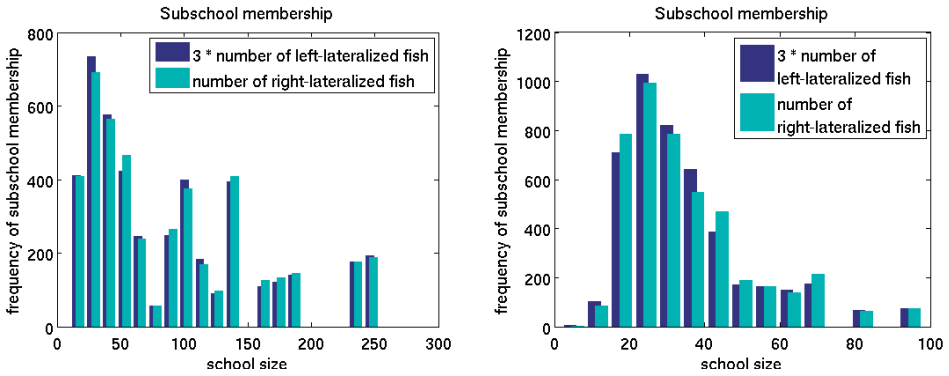

(a) No lateralization.

(b) Lateralization of 0.2

Figure 3.30: Histograms of subschool sizes for a minority fraction of 0.25 and majority fraction of 0.75. To be able to compare the two, the frequencies of the minority have been multiplied by 3.

3.3 Experiment 3: Stability based on school size and lateralization strength

The previous experiment indicated that school stability is dependent on school size and lateralization strength. To further investigate this, we perform another experiment.

3.3.1 Design

A school is initialized by placing all fish randomly in a space proportional to the number of individuals in the school. As in experiment 2, the lateralized fractions are fixed, but the fractions are different this time. Instead of the 3-to-1-ratio of experiment 2, the school consists of equal ratios of left- and right-lateralized individuals. We look at combinations of school sizes and lateralization strength. School size is varied from 20 to 200 individuals and lateralization strength from 0 to 0.4. All other parameters are kept the same as in experiment 2.

Stability of a school is tested by simulating it for (at most) 5 simulated minutes. If the school breaks up before that time we consider it unstable, otherwise we consider the school stable. Per combination of school size and lateralization strength, we perform 20 runs and count the number of stable schools.

3.3.2 Results

The results of the experiment are plotted in figure 3.31.

Due to the low number of simulation instances, there is some variation in the original data (figure 3.31a). To show the dependences more clearly, a blur was applied to average out these variations (figure 3.31b). We see that schools of 20 individuals are very stable regardless of lateralization strength (in the inspected range). This is because 'information' travels very fast in this school, relative to the size of the school.

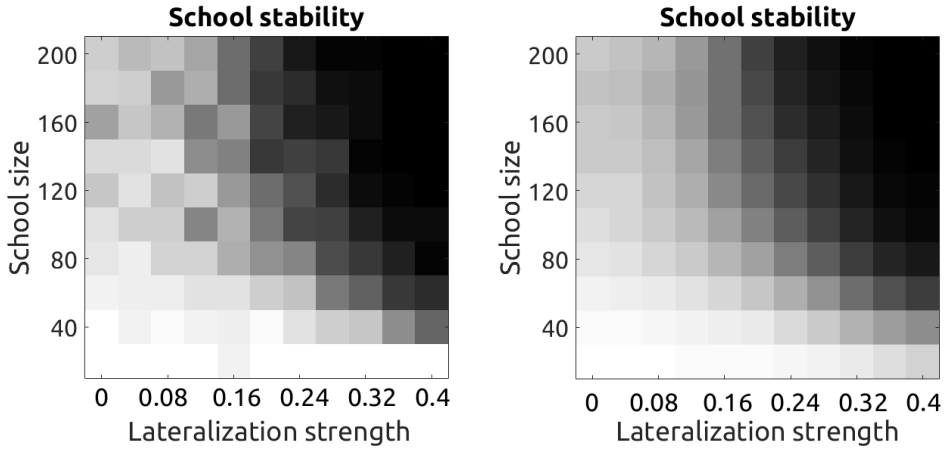

(a) Original data.

(b) After box blur.

Figure 3.31: Stability as a function of school size and lateralization strength. Light areas represent high stability, dark areas represent low stability.

As the number of individuals increases, the time it takes for information to spread increases. So it happens that different parts of the school randomly move in separate directions, and the cohesive interactions that should bring them back together propagate too slowly through the school to prevent a breakup. For lateralization strength we see a similar influence: with no lateralization, schools of all sizes are quite stable. As lateralization increases, schools become more unstable. This appears to be because in repulsive neighbor interactions between neighbors of the same lateralization, one of the interacting neighbors makes a large turn away, while the other makes a relatively small turn. Since we have both lateralizations in the school, the large turns are made in both directions, resulting in more chaotic schooling behavior. Chaotic (i.e., unpolarized) schooling behavior increases school instability quite directly, but it also leads to broadening of the school (through the same mechanism that causes assortment in more stable schools). In these broader schools, the time for information to travel from one side to the other increases, so that breakups more easily occur.

4. Discussion

4.1 Time complexity of the neighbor search

We did not find any references on the complexity of grid-based neighbor searches, but it is doubtful whether such an analysis would be applicable to our particular algorithm. We will not treat the time complexity of the box search in a completely formal manner, but the following argument should give a good estimate of the expected time complexity.

The box search allows each fish to search in its neighborhood, and in a typical case it has to consider only a small number of fish. The important consequence of searching a local neighborhood is that searching time of an individual fish no longer scales linearly with the total number of fish N. In fact, if we were to subdivide our space in all three dimensions with an appropriate box size, searching for a single nearest neighbor would take approximately $\mathcal{O}(1)$ time if fish are somewhat homogeneously distributed in space. Since our space is not subdivided in the z-direction (due to memory limitations), the search time for a single neighbor does increase with the total number of fish. Specifically, the expected search time for a single neighbor would be $\mathcal{O}(N^{1/3})$, for a school that scales uniformly. As we have seen, the shape of our school changes with increasing school size, but the increase in length is largely compensated by a relative decrease in width. This means that our box search will probably have time complexity of around $\mathcal{O}(N^{1/3})$. Because all other aspects of the simulation scale linearly with the number of fish, the expected time complexity of our simulation will be limited by $\mathcal{O}(N^{4/3})$. Note that as in all grid-based algorithms, the theoretical worst case complexity is still $\mathcal{O}(N^2)$ since all the fish in the school could form a 'pillar' in a single box.

The time complexity also depends on our choice of the box size. The box size influences how many fish there will be per box, and how many boxes we need to consider before we can stop the search. This is however no performance concern, since we can freely set the size of the boxes to be optimal.

We tested the performance of our program for school sizes between 50 and 600, simulating one hour of schooling time for each setting. Computation times are plotted in figure 4.1. As we expected, computation time goes approximately as $N^{4/3}$ in the range under study.

All things considered, the time complexity is acceptable for our purposes and we are mostly limited by the number of experiments and amount of time we wish to simulate. The final results of this thesis are based on nearly 200 hours of schooling time, with school sizes that are relatively high, compared to most of the literature.

4.2 School size experiments

Since we have been unable to find simulation studies with lateralization in the literature, we will focus on our school size experiment. For this, we mostly look at Hemelrijk and Hildenbrandt [2008] and Hemelrijk et al. [2010] since we found no other work that treated sufficient numbers of fish.

Our nearest neighbor distance increases with school size. Reuter and Breckling [1994] got a different result from their simulations, namely that nearest neighbor distance decreases between 10 and 20 individuals, but is almost constant after that up to 60 individuals. Our results are also different from what Hemelrijk et al. [2010] found using a model and empirical observations of relatively small schools (up to

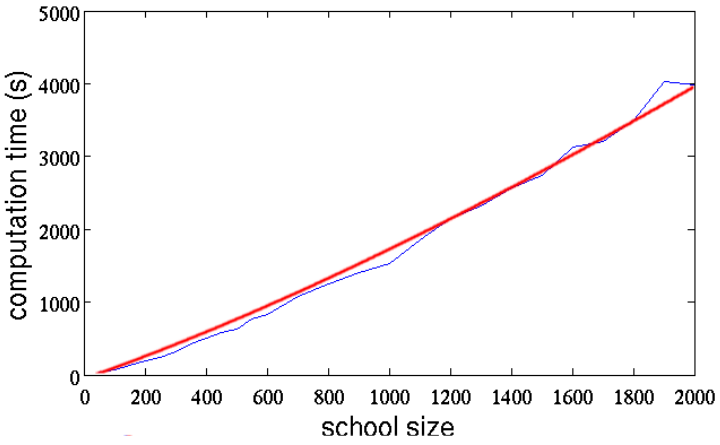

Figure 4.1: Computation times of one hour of simulated schooling time for various school sizes. The red line shows the theoretical $N^{4/3}$-dependence.

60 individuals) in a circular tank. Their results show decreasing nearest neighbor distance up to about 40 individuals, after which it stays more constant. The small school size and tank environment make it difficult to compare these results to ours.

Hemelrijk and Hildenbrandt [2008] report school density. This is calculated for an individual from the number of neighbors in its cohesion range, and from its nearest neighbor distance. Density increases quite strongly with school size in their model, so nearest neighbor distance surely decreases - the opposite result from our findings.

There are two differences between our model and that of Hemelrijk and Hildenbrandt [2008] that may explain this.

Firstly, in the model of Hemelrijk and Hildenbrandt [2008], each fish calculates a single cohesive force and a single separating force from all its neighbors. The separating force is only slightly stronger than the cohesive force (10N versus 9N). This is different from our model, where each neighbor makes an individual contribution to the total turning response. In our model, the cohesive contributions of all influential neighbors tend to cancel out, and the weight of a separating interaction is much stronger than that of a cohesive one. In addition, if multiple neighbors are in the separation zone, Hemelrijk and Hildenbrandt [2008] calculate a single separating force from both these neighbors. In our model, all neighbors in the separation zone contribute high weights to the positional interaction, quickly outweighing the cohesive forces from other neighbors. Consequently, in our model, fish inside the school are 'trying' much harder to keep a certain distance to their neighbors. The 'pressure' on the school of fish near the edge may be comparable in our model and that of Hemelrijk and Hildenbrandt [2008], but the school of Hemelrijk and Hildenbrandt [2008] is much more 'compressible'.

A second difference that may be important is that in the work of Hemelrijk and Hildenbrandt [2008], fish typically have a higher number of influential neighbors. A first concern we might have (but which, as we will explain below, is unwarranted), is that with a high number of neighbors, the spacing between fish may break down. This was found by Parrish et al. [2002], in schools of sizes between 16 and 24 individuals. However, in the model of Parrish et al. [2002] each influential neighbor causes a separate force. This gives much more importance to cohesion as more neighbors

are added. Thus, for a high number of influential neighbors, the separating force is dwarfed by the cohesive force, leading to an irregular spacing of fish. In the model of Hemelrijk and Hildenbrandt [2008], more neighbors only lead to a change in direction of the cohesive force, which points to the center of mass of all cohesive neighbors. It is therefore very unlikely that such a breakdown of regular spacing would occur for Hemelrijk and Hildenbrandt [2008].

The high number of neighbors in the model of Hemelrijk and Hildenbrandt [2008] has a consequence that does matter though: near the edge of the school, a thicker layer of fish is attracted into the school. To understand this, consider a fish with an adaptive radius that is greater than its distance to the edge of the school. This fish will have less influential neighbors in the direction of the edge of the school, since there is some 'empty space' in its perception range, outside the school. The center of mass of its neighbors will then be located away from the edge of the school, and the cohesive force on the focal fish will point away from the edge. A high number of influential neighbors typically corresponds to a large adaptive radius. With large adaptive radii, there will be a greater number of fish that is attracted toward the center of the school. Moreover, all these attracted fish have the same cohesive force, since the magnitude of this force is constant in the model of Hemelrijk and Hildenbrandt [2008].

In contrast, in our model the fish have relatively few neighbors, so that there is a relatively small layer of fish near the edge that is attracted into the school. Also, the cohesive 'force' on these fish is not constant, but becomes weaker the further into the school they are located. This is because in our model, a focal fish that is located somewhat into the school may be attracted by fish that are closer to the edge of the school.

In conclusion, the model of Hemelrijk and Hildenbrandt [2008] probably shows an increase in density with increasing school size because their school is more easily compressible, and a thicker layer of fish exerts pressure on the school.

Our polarization increases between 20 and 200 individuals, and is lower for 1000 and 2000 individuals. This is different from the result of Reuter and Breckling [1994], who have weakly decreasing polarization for schools of up to 60 individuals. Our result is also different from that of Hemelrijk and Hildenbrandt [2008], whose polarization is weakly decreasing. This can be explained by recalling that our result for nearest neighbor distance is also opposed to the result of Hemelrijk and Hildenbrandt [2008]. In the case of Hemelrijk and Hildenbrandt [2008], nearest neighbor distance decreases with school size, so that, as they explain, fish spend more time avoiding collisions. This causes them to be less aligned with each other. In our results we have the opposite dependence: nearest neighbor distance increases with school size, leading to better alignment between the fish.

We note that the polarization as found by Hemelrijk and Hildenbrandt [2008] is generally higher than ours (at least 0.995, compared to our highest value of 0.99). The difference may be because our school has some fish doing 'loopings', which decreases polarization, but it is more likely because the model of Hemelrijk and Hildenbrandt [2008] has relatively stronger alignment than our model.

A result that seems to confirm the above argument that higher nearest neighbor distance results in higher polarization of the school is given by Huth and Wissel [1994]. They reported a positive correlation between nearest neighbor distance and polarization for schools of 20 and 100 individuals.

Our frontality is mostly higher than 0.5, meaning the dense core is positioned toward the front of the school. This is in agreement with frontality as found by Hemelrijk and Hildenbrandt [2008], but the dependence is different. Our frontality decreases with school size, while frontality clearly increases according to Hemelrijk

and Hildenbrandt [2008]. This can be explained by comparing frontality with nearest neighbor distance and polarization: with increasing school size, nearest neighbor distance and polarization both increase. The low nearest neighbor distance leads to more zigzag movement (low polarization) and more acceleration and deceleration to avoid collisions. This leads to a 'traffic jam' of high density, as described by Hemelrijk and Hildenbrandt [2008], at the front of the school. At the back of the school, it is easier for fish to regulate their nearest neighbor distance, because fish can easily increase nearest neighbor distance by decelerating. Near the front, it is not as easy to adjust nearest neighbor distance through acceleration for two reasons. Firstly, the blind angle behind fish means that sometimes a neighbor that would cause such an acceleration is not visible (compare the near speeding areas of figure 2.4). Secondly, if a fish accelerates, it is attracted to neighbors on the left or on the right, either leading to a zigzag movement that will, as we discussed, slow down the net forward movement of the fish, or to a flaking manoeuvre.

Our length-over-width ratio increases with school size, and is quantitatively very similar to the result of Hemelrijk and Hildenbrandt [2008], except for our 'outlier' of school size 10. Hemelrijk et al. [2010] confirmed lengthening of schools with school size up to 60 individuals in a circular fish tank. It should be noted that we can easily change the length-over-width ratio of our school by varying the parameters of the speedup interaction, as discussed in section 2.2.1.

Some of the data obtained from our experiments (with large unlateralized schools) shows quite persistent schools; the schools made few turns and could move in straight lines for hundreds of body lengths. This may be somewhat surprising, considering that the fish in the school would turn quite a lot, as we can tell from their polarization and relative movement. For comparison we looked at Tikhonov et al. [2001], who studied the movement of fish schools interacting with plankton (their food source). Their (simulated) fish schools also tend to swim in straight lines for long distances, and their turning can mostly be attributed to the interaction with plankton. Unfortunately, we did not find suitable empirical data on the trajectories of fish schools.

Our present comparisons show some different results from those in the literature. As Parrish et al. [2002] noted, different modelling approaches frequently lead to seemingly contradictory conclusions. Since most models, including ours, are supposed to model general fish-like behavior, there is no 'gold standard' to compare results with (and in reality, even a single species exhibits different schooling patterns depending on the circumstances). Consequently, it is hard to tell whether the mechanisms of the model reflect any biological reality. It may seem disheartening that even small changes in a model, to any of its parameters or mechanisms can have large consequences for its emergent schooling behavior. The large size of our 'parameter space' means that it is unlikely that we can predict schooling behavior purely by evaluating a set of individual rules. However, as long as we can point out the mechanisms through which certain patterns occur, we gain at least some insight for explaining observed phenomena.

4.3 Lateralization experiments

The key characteristic of lateralization in our model is that it gives an individual a turning bias. For schools of uneven fractions of left- and right-lateralized individuals, this means that the school as a whole has a turning bias. Unfortunately, no mention of this was found in the literature. This is not surprising for several reasons:

1. Our mechanism of lateralization is very simple, so it would be optimistic to

expect that our model would accurately reflect lateralization in real fish. As previously explained, the turning bias probably arises because the direction of lateralized fish is determined mostly through repulsive interactions. Preliminary simulations resulted in a turning bias in the other direction (presumably with cohesion causing the bias). We must conclude from this that it is possible to create a model with population-level lateralization in which no turning bias is present at all. Nevertheless, it was empirically demonstrated (as mentioned in the introduction) that lateralized fish prefer to have a neighbor on one side rather than the other. This does make it conceivable that schools in nature that have uneven fractions of lateralized fish have some turning bias.

2. Schools in nature have many other impulses that could easily outweigh any turning bias such as searching for food (Tikhonov et al. [2001]), water currents, natural obstacles and optimizing swimming efficiency (Weihs [1975], Stöcker [1999]).

3. Even if schools with population-level lateralization have a turning bias, it is quite difficult to study this empirically. One would need to somehow mark a stable school and be able to track it over time. The turning bias may also be very weak.

Our experiments with lateralized fraction reveal non-monotonic dependencies for frontality and length-over-width. Without making any guesses about evolutionary mechanisms, this in itself shows that certain metrics of schools (in our results: polarization, frontality and length-over-width) may be optimized through intermediate population-level lateralization.

Our last experiment also shows that stronger individual lateralization leads to smaller schools. This would typically reduce the safety-in-numbers-advantage that fish are supposed to have by schooling. Lateralization strength could therefore be determined by an optimal balance between school stability and the advantages of lateralization as discussed in the introduction.

5. Future Work

Several directions remain to be explored:

1. Lateralized fish have a turning bias due to dominance of separation over cohesion, according to our model. It would be great to know what the conditions for this behavior are. Could one neutralize or reverse this turning bias?

2. Does lateralization change the likelihood of state transitions between schooling and milling? These transitions have been studied in practice by Tunstrøm et al. [2013] and in simulations by Calovi et al. [2014] and make good case studies for lateralization.

3. The experiment with unstable schools shows no correlation between the size of an individuals subschool and its (majority/minority) lateralization. In more stable schools this may be different, since the two lateralizations need some time to assort themselves. If the school breaks up after being sorted, it is quite probable that there exists some correlation between the lateralization type (minority or majority) of a fish and the expected size of the subschool that it occupies. Unfortunately, experiment to test this would take a long time, especially since there is a lot of uncertainty in the breaking up of schools (as is evident from figure 3.29).

4. In our first experiment, with varying school size, our metrics have very different values for 10 fish, compared to larger schools. A more detailed study of the range from 1 to 20 individuals could reveal how the transition in behavior from small to larger schools occurs in our model.

5. The influence of various types of predators could be tested to see whether lateralization has an influence on escape success of prey.

6. For further progress with simulations, it is necessary to collect more empirical data. For the results presented in this thesis it would be most interesting to know whether schools with unequal numbers of left- and right-lateralized fish (ideally schools of only one lateralization type) exhibit a turning bias.

Appendices

A. Flattening of the school

In the first version of our model, the school quickly became very flat for high (>200) numbers of fish. The obvious explanation was that this flattening was caused by the horizontal stabilization. This is after all the most obvious, explicit breaker of symmetry between the vertical and horizontal directions. Surprisingly, disabling horizontal stabilization did not resolve the issue: the school still instantly got into a flat formation. This result was however in agreement with Hemelrijk and Hildenbrandt [2008], in which a comparable kind of horizontal stabilization is used, and quite spherical schools are reported.

The true cause of the flattening turned out to be a less conspicuous symmetry breaker in the model: the division of the visual fields into left and right regions, in particular the fixed number of neighbors that each eye can perceive. This hypothesis was verified by setting both eyes to have full vision confirmed this suspicion; even with horizontal stabilization enabled, the school remained quite spherical. Our initial explanation (which, as we shall see further on, is only part of the whole explanation) for this was that the fish above and below the school try to interact with twice as many neighbors as those on the sides (namely, the same number but with each eye). This causes the above-and-below fish to also interact with fish that are further away, deeper into the school. Since these interactions are cohesive, these fish tend to be attracted toward the school more, leading to a higher 'pressure' on the school from the top and bottom than from the sides. This of course leads to a flat school.

One attempted solution was to limit the total number of neighbors instead of the number per eye, while trying to balance the numbers of left and right neighbors. The method for this is shown in the pseudocode of listing A.1. Unfortunately, this attempt did not bear fruit; the school still flattened out very much.

Listing A.1: Pseudocode for discarding nearest neighbors.

```
1  while total neighbors > total neighbors allowed
2    if more left than right
3      discard farthest left neighbor
4    else if more right than left
5        discard farthest right neighbor
6    else // Left and right have equal nr of neighbors
7      if distance farthest left > distance farthest right
8        discard farthest left neighbor
9      else
10       discard farthest right neighbor
11     end if
12   end if
13 end while
```

A first possible explanation for this was that fish above and below the school do not always interact with only *nearest* visible neighbors, while fish that swim next to the school do. The further away neighbors of above-or-below fish would then more often be attractive than the true nearest visible neighbors of the fish next to the school.

The problem with this explanation is that all but the closest fish are attractive. It is therefore highly unlikely that cases occur where more than 2 or 3 neighbors are repulsive. Any further away neighbors are attractive anyway, whether they are 'nearest' or not.

Another possible explanation was the blind angle of 30 degrees above and below the fish. This causes them to sometimes ignore nearest neighbors that would indeed be close enough to be repulsive - if they would be perceived. A short experiment with a full vertical viewing angle refuted this hypothesis too, the school still flattened out.

The real explanation seems to be more complex than the ones discussed above. Consider a fish left of the school, perceiving neighbors only with its right eye. If this fish turns away (due to a repulsive interaction with a neighbor), it will start to perceive neighbors behind it with its left eye. If we use our 'greedy' balancing strategy (listing A.1), all rear neighbors entering the field of vision of the left eye will give the fish a tendency to turn left, reinforcing the turning away from the school.

The same mechanism does not apply to a fish swimming above the school. If it pitches upward, some neighbors behind it might indeed cause it to pitch even more (making a looping). However, both eyes of the focal fish likely see more neighbors below it that would counter the effect (i.e., change pitch toward the school again through cohesion). For this reason, the neighbors that would cause pitching away from the school will only make a small contribution to the total turning of the focal fish. Since the sides of the school move away more easily than the top and bottom, the school flattens out.

The above explanation is less straightforward to test. One observation that seems to confirm it is based on the alignment parameter: consider again the fish on the left of the school. When this fish turns away, it perceives new neighbors behind it with its left eye. These neighbors cause a higher tendency to make a 'looping' through the positional interaction. However, these neighbors also cause a tendency to turn back toward the school through the alignment interaction. Therefore we expect the flattening to be weaker if we increase the alignment parameter. A short experiment confirmed this, the school did not flatten out while still being quite dynamic. We also changed the model to give greater weight to fish that are in front of the focal fish, but this had the side effect of also increasing confusion and making the school more longitudinal. There seemed to be less flattening, but due to the different dynamics, it is hard to tell through which mechanism.

B. Full results of experiment 1

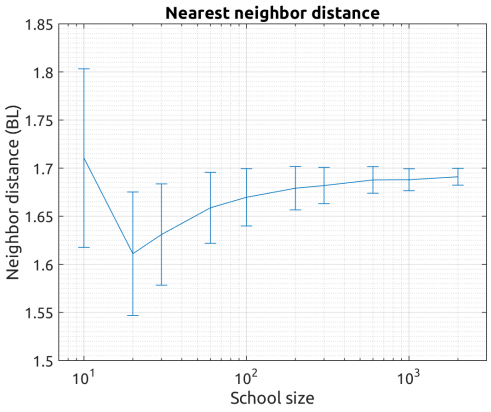

(a) Average nearest neighbor distance.

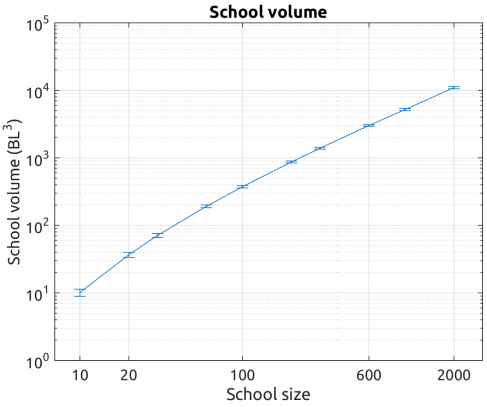

(b) Average volume of the school, calculated from its alpha shape with $\alpha = 1/4$.

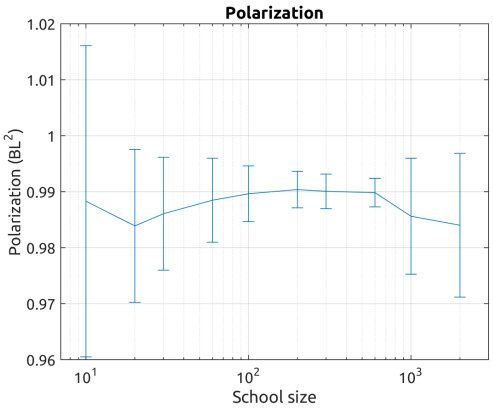

(c) Average polarization.

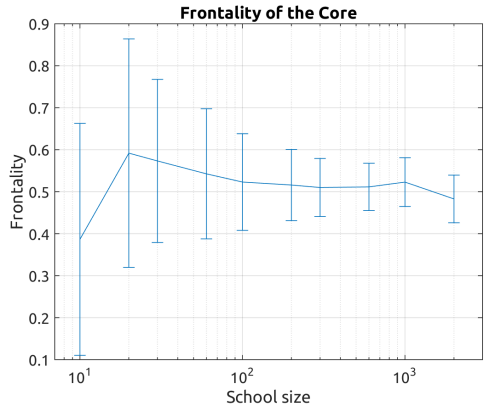

(d) Frontality of the core.

Figure B.1: Results of the 8-influential neighbors experiment of varying school sizes. Lateralization was disabled in this experiment.

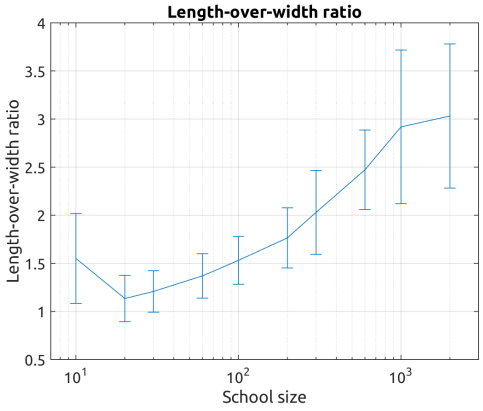

(a) Average length-over-width ratio.

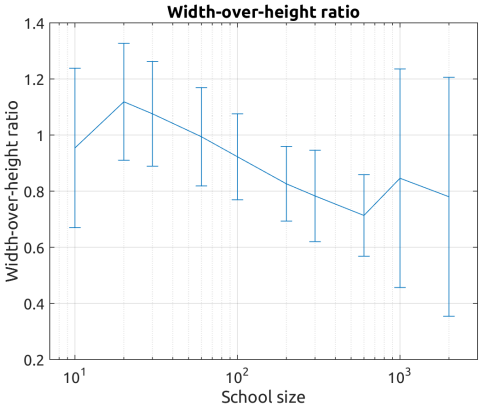

(b) Average width-over-height ratio.

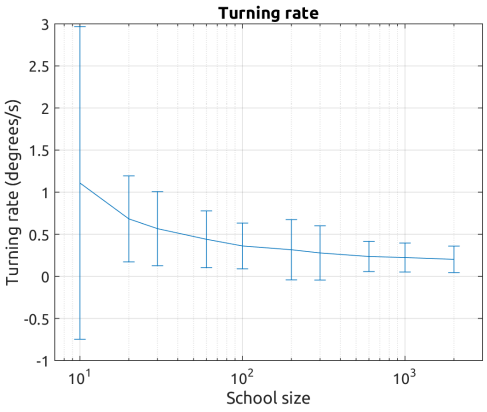

(c) Turning rate, calculated from center of mass at 10 second intervals.

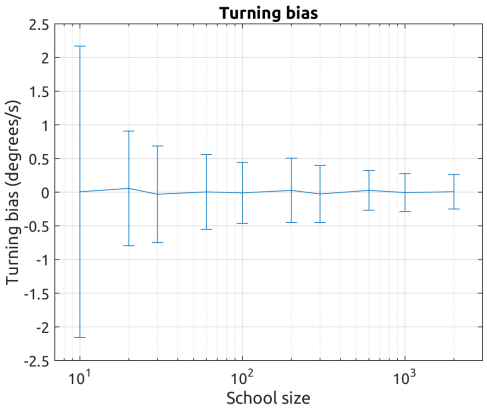

(d) Turning bias. Calculated from center of mass at 10 second intervals.

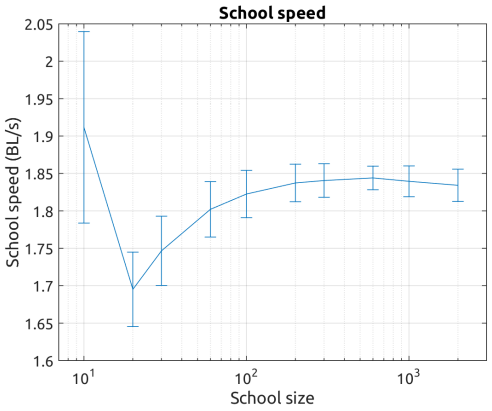

(e) Average school speed, calculated from center of mass displacements at 10 second intervals.

Figure B.2: Results of the 8-influential neighbors experiment of varying school sizes. Lateralization was disabled in this experiment.

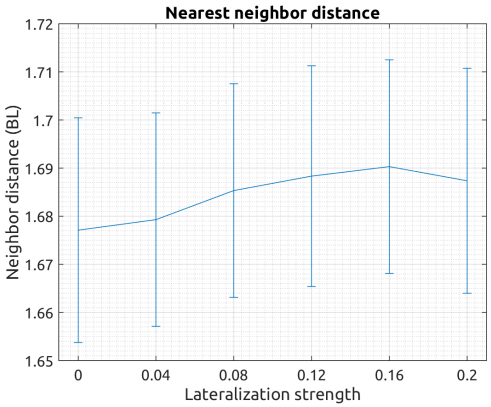

(a) Average nearest neighbor distance.

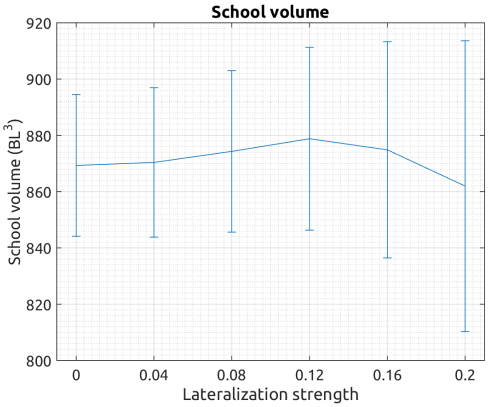

(b) Average volume of the school, calculated from its alpha shape with $\alpha = 1/4$.

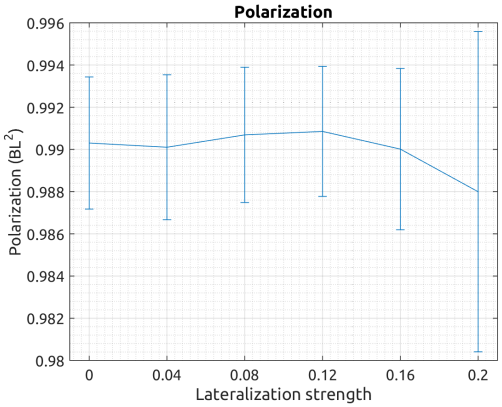

(c) Average polarization.

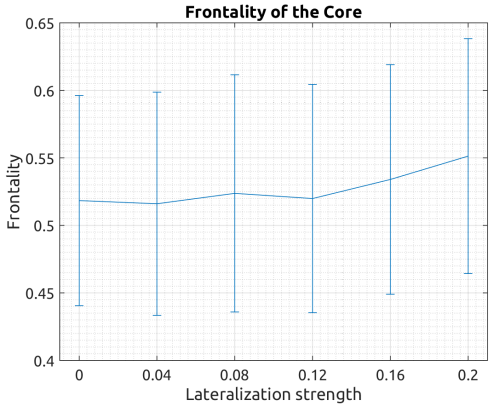

(d) Frontality of the core.

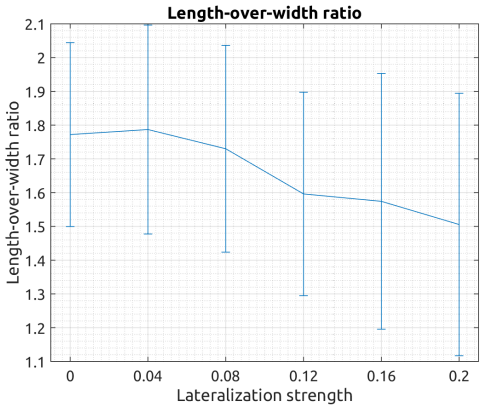

(e) Average length-over-width ratio.

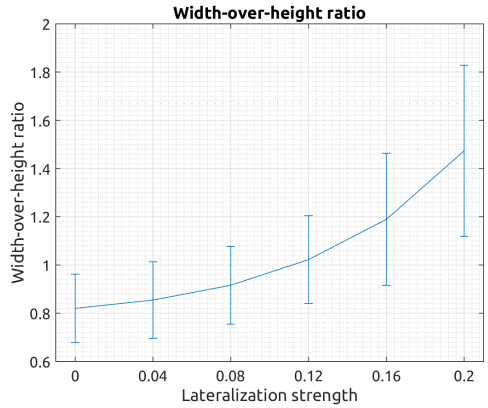

(f) Average width-over-height ratio.

Figure B.3: Results of the 8-influential neighbors experiment of varying lateralization strength.

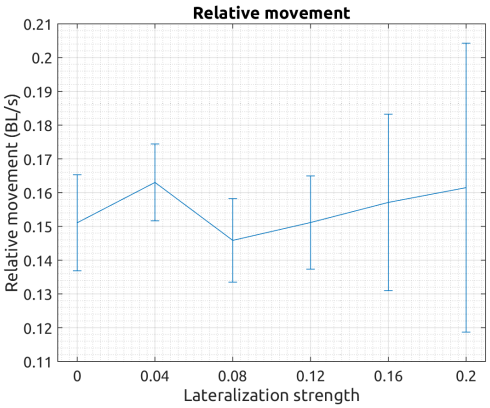

(a) Relative movement. Calculated for each fish using the relative displacement of the 3 nearest neighbors.

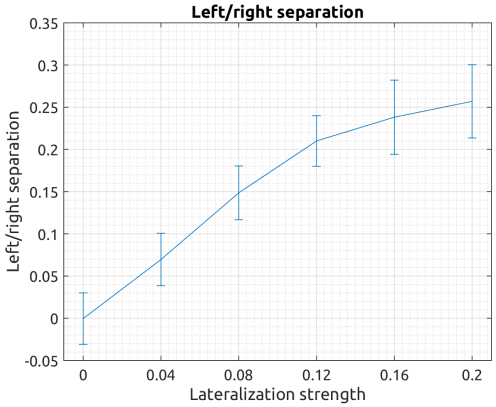

(b) Left/right separation.

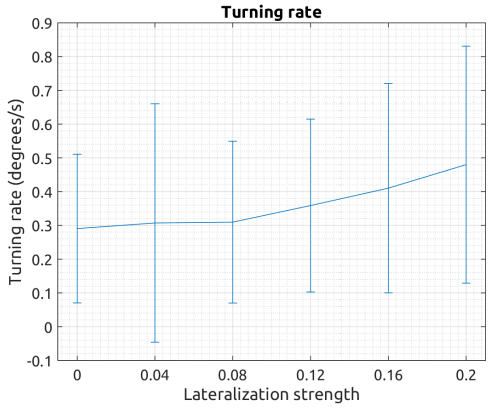

(c) Turning rate, calculated from center of mass at 10 second intervals.

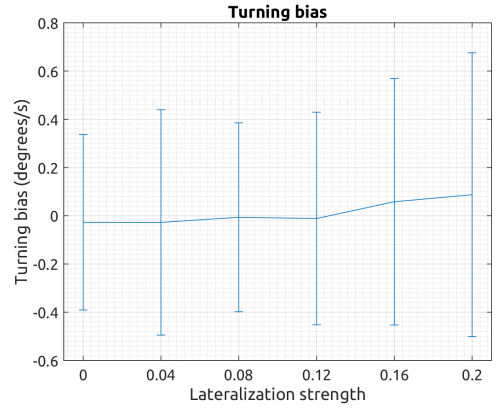

(d) Turning bias. Calculated from center of mass at 10 second intervals.

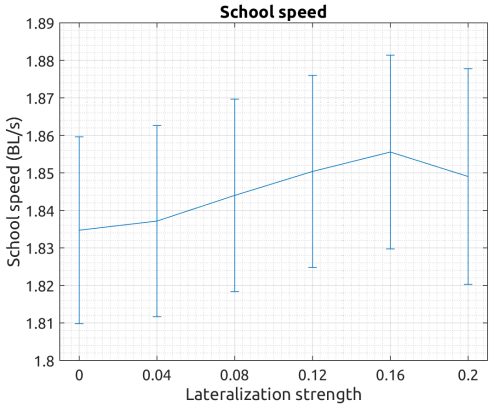

(e) Average school speed, calculated from center of mass displacements at 10 second intervals.

Figure B.4: Results of the 8-influential neighbors experiment of varying lateralization strength.

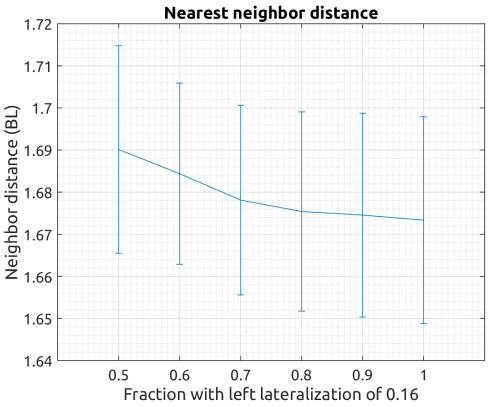

(a) Average nearest neighbor distance.

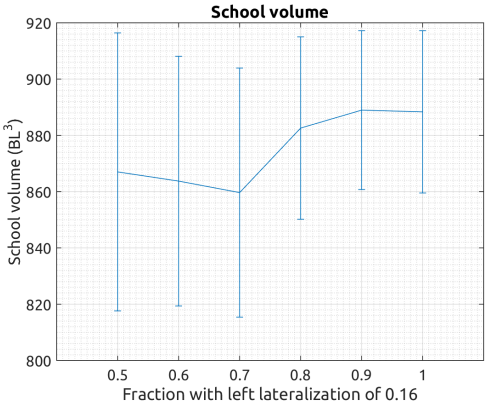

(b) Average volume of the school, calculated from its alpha shape with $\alpha = 1/4$.

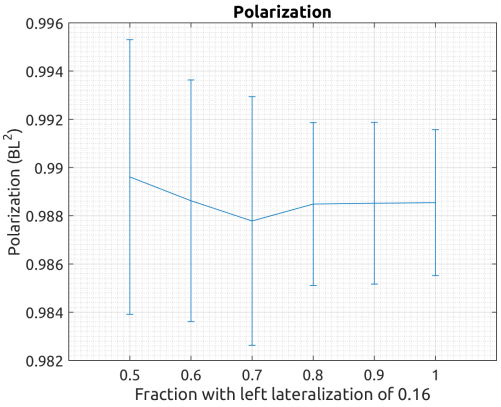

(c) Average polarization.

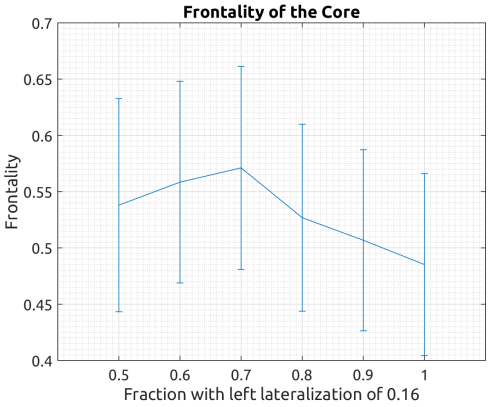

(d) Frontality of the core.

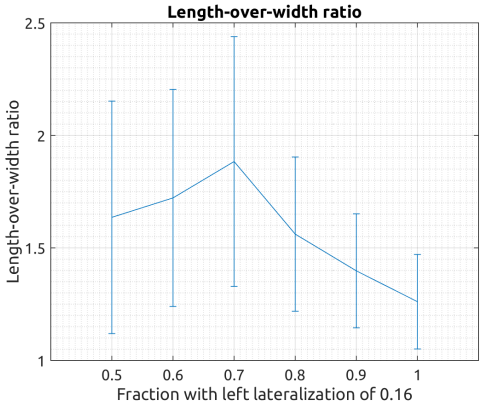

(e) Average length-over-width ratio.

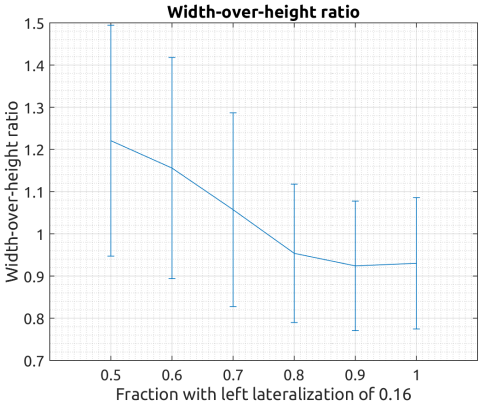

(f) Average width-over-height ratio.

Figure B.5: Results of the 8-influential neighbors experiment with 200 individuals and varying left-lateralized fraction with lateralization strength 0.16.

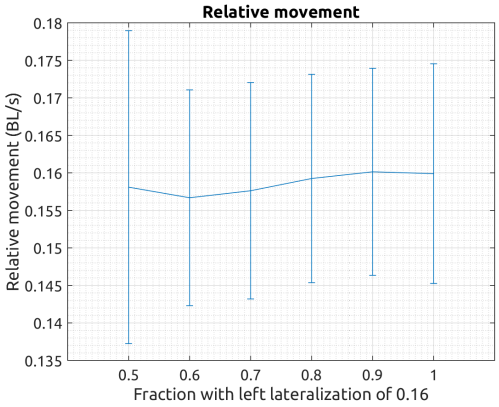

(a) Relative movement. Calculated for each fish using the relative displacement of the 3 nearest neighbors.

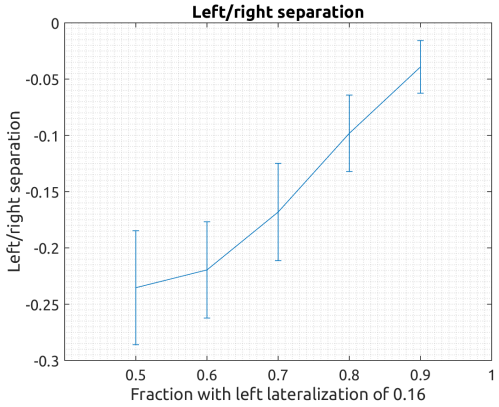

(b) Left/right separation.

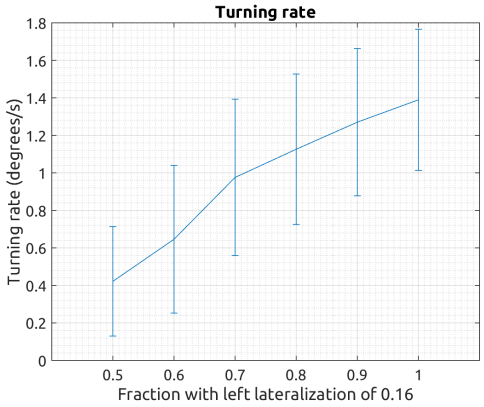

(c) Turning rate, calculated from center of mass at 10 second intervals.

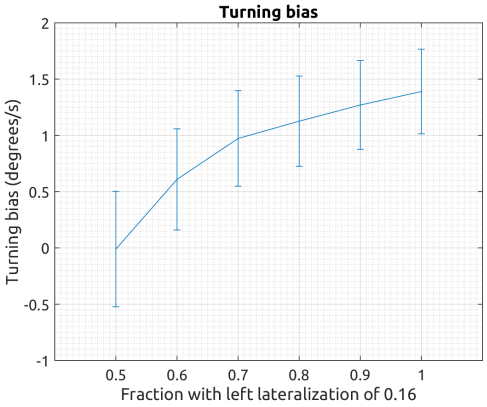

(d) Turning bias. Calculated from center of mass at 10 second intervals.

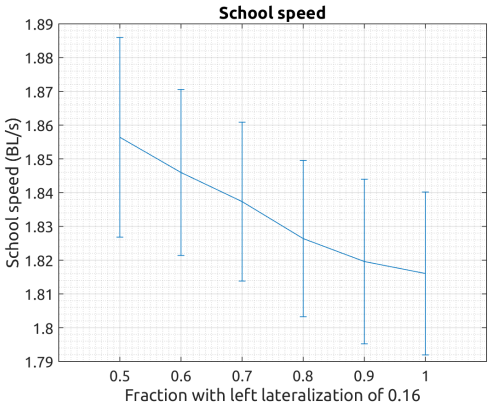

(e) Average school speed, calculated from center of mass displacements at 10 second intervals.

Figure B.6: Results of the 8-influential neighbors experiment with 200 individuals and varying left-lateralized fraction with lateralization strength 0.16.

Bibliography

Bisazza, A., Cantalupo, C., Capocchiano, M., and Vallortigara, G. (2000). Population lateralisation and social behaviour: a study with 16 species of fish. *Laterality: Asymmetries of Body, Brain and Cognition*, **5**(3), 269–284.

Bisazza, A., De Santi, A., and Vallortigara, G. (1999). Laterality and cooperation: mosquitofish move closer to a predator when the companion is on their left side. *Animal Behaviour*, **57**(5), 1145–1149.

Bisazza, A., Rogers, L. J., and Vallortigara, G. (1998). The origins of cerebral asymmetry: a review of evidence of behavioural and brain lateralization in fishes, reptiles and amphibians. *Neuroscience & Biobehavioral Reviews*, **22**(3), 411–426.

Bisazza, A., Sovrano, V. A., and Vallortigara, G. (2001). Consistency among different tasks of left–right asymmetries in lines of fish originally selected for opposite direction of lateralization in a detour task. *Neuropsychologia*, **39**(10), 1077–1085.

Calovi, D. S., Lopez, U., Ngo, S., Sire, C., Chaté, H., and Theraulaz, G. (2014). Swarming, schooling, milling: phase diagram of a data-driven fish school model. *New Journal of Physics*, **16**(1), 015026.

Couzin, I. D., Krause, J., James, R., Ruxton, G. D., and Franks, N. R. (2002). Collective memory and spatial sorting in animal groups. *Journal of theoretical biology*, **218**(1), 1–11.

De Santi, A., Sovrano, V., Bisazza, A., and Vallortigara, G. (2001). Mosquitofish display differential left-and right-eye use during mirror image scrutiny and predator inspection responses. *Animal Behaviour*, **61**(2), 305–310.

Gautrais, J., Jost, C., et al. (2009). Analyzing fish movement as a persistent turning walker. *Journal of mathematical biology*, **58**(3), 429–445.

Ghirlanda, S. and Vallortigara, G. (2004). The evolution of brain lateralization: a game-theoretical analysis of population structure. *Proceedings of the Royal Society of London-B*, **271**(1541), 853–858.

Glick, S. (2012). *Cerebral lateralization in nonhuman species*. Elsevier.

Hearn, D. and Baker, M. P. (1997). *Computer graphics, C version*. Prentice Hall Upper Saddle River.

Hemelrijk, C. K. and Hildenbrandt, H. (2008). Self-organized shape and frontal density of fish schools. *Ethology*, **114**(3), 245–254.

Hemelrijk, C. K., Hildenbrandt, H., Reinders, J., and Stamhuis, E. J. (2010). Emergence of oblong school shape: models and empirical data of fish. *Ethology*, **116**(11), 1099–1112.

Hemelrijk, C. K. and Kunz, H. (2005). Density distribution and size sorting in fish schools: an individual-based model. *Behavioral Ecology*, **16**(1), 178–187.

Huth, A. and Wissel, C. (1992). The simulation of the movement of fish schools. *Journal of theoretical biology*, **156**(3), 365–385.

Huth, A. and Wissel, C. (1994). The simulation of fish schools in comparison with experimental data. *Ecological Modelling*, **75**, 135–146.

Kalashnikov, D. V., Prabhakar, S., and Hambrusch, S. E. (2004). Main memory evaluation of monitoring queries over moving objects. *Distributed and Parallel Databases*, **15**(2), 117–135.

Katz, Y., Tunstrøm, K., Ioannou, C. C., Huepe, C., and Couzin, I. D. (2011). Inferring the structure and dynamics of interactions in schooling fish. *Proceedings of the National Academy of Sciences*, **108**(46), 18720–18725.

Korn, F., Sidiropoulos, N., and Faloutsos, C. (1996). Fast nearest neighbor search in medical image databases.

Kunz, H. and Hemelrijk, C. K. (2003). Artificial fish schools: collective effects of school size, body size, and body form. *Artificial life*, **9**(3), 237–253.

Levy, J. (1977). The mammalian brain and the adaptive advantage of cerebral asymmetry. *Annals of the New York Academy of Sciences*, **299**(1), 264–272.

Møller, A. P. and Swaddle, J. P. (1997). *Asymmetry, developmental stability and evolution, 2nd edition*. Oxford University Press, UK.

Parrish, J. K., Viscido, S. V., and Grünbaum, D. (2002). Self-organized fish schools: an examination of emergent properties. *The biological bulletin*, **202**(3), 296–305.

Partridge, B. L., Pitcher, T., Cullen, J. M., and Wilson, J. (1980). The three-dimensional structure of fish schools. *Behavioral Ecology and Sociobiology*, **6**(4), 277–288.

Partridge, B. L. and Pitcher, T. J. (1980). The sensory basis of fish schools: relative roles of lateral line and vision. *Journal of Comparative Physiology*, **135**(4), 315–325.

Reuter, H. and Breckling, B. (1994). Selforganization of fish schools: an object-oriented model. *Ecological Modelling*, **75**, 147–159.

Rogers, L. J. (2000). Evolution of hemispheric specialization: advantages and disadvantages. *Brain and language*, **73**(2), 236–253.

Rogers, L. J. (2012). The two hemispheres of the avian brain: their differing roles in perceptual processing and the expression of behavior. *Journal of Ornithology*, **153**(1), 61–74.

Romey, W. L. (1996). Individual differences make a difference in the trajectories of simulated schools of fish. *Ecological Modelling*, **92**(1), 65–77.

Roussopoulos, N., Kelley, S., and Vincent, F. (1995). Nearest neighbor queries. In *ACM sigmod record*, vol. 24, 71–79. ACM.

Roy, A. E. (2012). *Predictability, stability, and chaos in N-body dynamical systems*, vol. 272. Springer Science & Business Media.

Seidl, T. and Kriegel, H.-P. (1998). Optimal multi-step k-nearest neighbor search. In *ACM SIGMOD Record*, vol. 27, 154–165. ACM.

Sherry, D. F. and Schacter, D. L. (1987). The evolution of multiple memory systems. *Psychological review*, **94**(4), 439.

Solar, R., Suppi, R., and Luque, E. (2011). High performance distributed cluster-based individual-oriented fish school simulation. *Procedia Computer Science*, **4**, 76–85.

Sovrano, V. A., Bisazza, A., and Vallortigara, G. (2001). Lateralization of response to social stimuli in fishes: a comparison between different methods and species. *Physiology & behavior*, **74**(1), 237–244.

Stöcker, S. (1999). Models for tuna school formation. *Mathematical Biosciences*, **156**(1), 167–190.

Tikhonov, D., Enderlein, J., Malchow, H., and Medvinsky, A. B. (2001). Chaos and fractals in fish school motion. *Chaos, Solitons & Fractals*, **12**(2), 277–288.

Tunstrøm, K., Katz, Y., Ioannou, C. C., Huepe, C., Lutz, M. J., and Couzin, I. D. (2013). Collective states, multistability and transitional behavior in schooling fish. *PLoS Comput Biol*, **9**(2), e1002915.

Vabø, R. and Skaret, G. (2008). Emerging school structures and collective dynamics in spawning herring: A simulation study. *Ecological Modelling*, **214**(2), 125–140.

Vallortigara, G. and Rogers, L. J. (2005). Survival with an asymmetrical brain: advantages and disadvantages of cerebral lateralization. *Behavioral and brain sciences*, **28**(4), 575–588.

Videler, J. and Weihs, D. (1982). Energetic advantages of burst-and-coast swimming of fish at high speeds. *Journal of Experimental Biology*, **97**(1), 169–178.

Viscido, S. V., Parrish, J. K., and Grünbaum, D. (2005). The effect of population size and number of influential neighbors on the emergent properties of fish schools. *Ecological Modelling*, **183**(2), 347–363.

Warburton, K. and Lazarus, J. (1991). Tendency-distance models of social cohesion in animal groups. *Journal of Theoretical Biology*, **150**(4), 473–488.

Weihs, D. (1975). Some hydrodynamical aspects of fish schooling. In *Swimming and flying in nature*, 703–718. Springer.

Yu, X., Pu, K. Q., and Koudas, N. (2005). Monitoring k-nearest neighbor queries over moving objects. In *Data Engineering, 2005. ICDE 2005. Proceedings. 21st International Conference on*, 631–642. IEEE.

Zhao, J., Long, C., Xiong, S., Liu, C., and Yuan, Z. (2013). A new k nearest neighbours algorithm using cell grids for 3d scattered point cloud. *Elektronika ir Elektrotechnika*, **20**(1), 81–87.